



## OPEN ACCESS

## EDITED BY

Vijayakumar Velu,  
Emory University, United States

## REVIEWED BY

Nanda Kishore Routhu,  
Emory Vaccine Center, School of  
Medicine, Emory University,  
United States  
Anusmita Sahoo,  
Emory Vaccine Center, School of  
Medicine, Emory University,  
United States

## \*CORRESPONDENCE

John J. Zaunders  
j.zaunders@amr.org.au

<sup>†</sup>These authors have contributed  
equally to this work

## SPECIALTY SECTION

This article was submitted to  
Viral Immunology,  
a section of the journal  
Frontiers in Immunology

RECEIVED 31 August 2022

ACCEPTED 31 October 2022

PUBLISHED 05 December 2022

## CITATION

Phetsouphanh C, Khoo WH,  
Jackson K, Klemm V, Howe A,  
Aggarwal A, Akerman A,  
Milogiannakis V, Stella AO, Rouet R,  
Schofield P, Faulks ML, Law H,  
Danwilai T, Starr M, Munier CML,  
Christ D, Singh M, Croucher PI,  
Brirot-Turville F, Turville S, Phan TG,  
Dore GJ, Darley D, Cunningham P,  
Matthews GV, Kelleher AD and  
Zaunders JJ (2022) High titre  
neutralizing antibodies in response  
to SARS-CoV-2 infection require  
RBD-specific CD4 T cells that  
include proliferative memory cells.  
*Front. Immunol.* 13:1032911.  
doi: 10.3389/fimmu.2022.1032911

# High titre neutralizing antibodies in response to SARS-CoV-2 infection require RBD-specific CD4 T cells that include proliferative memory cells

Chansavath Phetsouphanh<sup>1</sup>, Weng Hua Khoo<sup>2,3</sup>,  
Katherine Jackson<sup>2</sup>, Vera Klemm<sup>1</sup>, Annett Howe<sup>1</sup>,  
Anupriya Aggarwal<sup>1</sup>, Anouschka Akerman<sup>1</sup>,  
Vanessa Milogiannakis<sup>1</sup>, Alberto Ospina Stella<sup>1</sup>,  
Romain Rouet<sup>2</sup>, Peter Schofield<sup>2</sup>, Megan L. Faulks<sup>2</sup>,  
Hannah Law<sup>1</sup>, Thidarat Danwilai<sup>4</sup>, Mitchell Starr<sup>4</sup>,  
C. Mee Ling Munier<sup>1</sup>, Daniel Christ<sup>2</sup>, Mandeep Singh<sup>2,3</sup>,  
Peter I. Croucher<sup>2</sup>, Fabienne Brirot-Turville<sup>5,6</sup>, Stuart Turville<sup>1</sup>,  
Tri Giang Phan<sup>2,3</sup>, Gregory J. Dore<sup>1,7</sup>, David Darley<sup>7</sup>,  
Philip Cunningham<sup>4</sup>, Gail V. Matthews<sup>1,7</sup>,  
Anthony D. Kelleher<sup>1,8†</sup> and John J. Zaunders<sup>4\*†</sup>

<sup>1</sup>Kirby Institute, University of New South Wales (UNSW), Sydney, NSW, Australia, <sup>2</sup>Garvan Institute of Medical Research, Sydney, NSW, Australia, <sup>3</sup>St. Vincent's Clinical School, Faculty of Medicine, University of New South Wales (UNSW) Sydney, Sydney, NSW, Australia, <sup>4</sup>NSW State Reference Laboratory for HIV, St. Vincent's Centre for Applied Medical Research, Sydney, NSW, Australia, <sup>5</sup>Brain and Mind Centre, Children's Hospital at Westmead, University of Sydney, Sydney, NSW, Australia, <sup>6</sup>Sydney Institute for Infectious Diseases, The University of Sydney, Sydney, NSW, Australia, <sup>7</sup>Department of Infectious Diseases, St. Vincent's Hospital, Sydney, NSW, Australia, <sup>8</sup>Department of Immunology, St Vincent's Hospital, Sydney, NSW, Australia

**Background:** Long-term immunity to SARS-CoV-2 infection, including neutralizing antibodies and T cell-mediated immunity, is required in a very large majority of the population in order to reduce ongoing disease burden.

**Methods:** We have investigated the association between memory CD4 and CD8 T cells and levels of neutralizing antibodies in convalescent COVID-19 subjects.

**Findings:** Higher titres of convalescent neutralizing antibodies were associated with significantly higher levels of RBD-specific CD4 T cells, including specific memory cells that proliferated vigorously *in vitro*. Conversely, up to half of convalescent individuals had low neutralizing antibody titres together with a lack of receptor binding domain (RBD)-specific memory CD4 T cells. These low antibody subjects had other, non-RBD, spike-specific CD4 T cells, but with more of an inhibitory Foxp3+ and CTLA-4+ cell phenotype, in contrast to the effector T-bet+, cytotoxic granzymes+ and perforin+ cells seen in RBD-specific memory CD4 T cells from high antibody subjects. Single cell transcriptomics of

antigen-specific CD4<sup>+</sup> T cells from high antibody subjects similarly revealed heterogeneous RBD-specific CD4<sup>+</sup> T cells that comprised central memory, transitional memory and Tregs, as well as cytotoxic clusters containing diverse TCR repertoires, in individuals with high antibody levels. However, vaccination of low antibody convalescent individuals led to a slight but significant improvement in RBD-specific memory CD4 T cells and increased neutralizing antibody titres.

**Interpretation:** Our results suggest that targeting CD4 T cell epitopes proximal to and within the RBD-region should be prioritized in booster vaccines.

#### KEYWORDS

SARS-CoV-2, neutralizing antibodies, CD4 T cells, CD4 function, proliferation

## 1 Introduction

The question of the protective efficacy of both convalescent and vaccine induced immunity to SARS-CoV-2 is of global significance. This is highlighted by the multiple waves of infections, with rates of population-wide protection against re-infection of only 50-80% protection during 2020, depending on age (1), or an estimated 60% protection against symptomatic re-infection with the immuno-evasive Omicron variant (2). In order to end the COVID-19 pandemic, a large proportion of the population will need to be immune to the virus (3), or at least, if they become infected, to develop an immune response which minimizes virus shedding, symptoms and onward transmission. Early studies concentrated on serum antibody levels in recovered COVID-19 patients, and in particular neutralizing antibodies, since it is believed that the most effective vaccines to viral infections are associated with the generation of neutralizing antibodies and mimic natural infection (4). The highest titres and affinities of such neutralizing antibodies are generally dependent on CD4 T follicular helper cell (T<sub>fh</sub>) interaction with B cells to generate class switching and affinity maturation by somatic hypermutation within germinal centres, in secondary lymphoid organs (5).

In SARS-CoV-2 infection, the longest study of neutralizing antibodies in convalescent patients from the original 2020 epidemic showed that neutralizing antibody titres peaked at 3-4 months after onset of symptoms, but just under half of patients still had detectable neutralizing antibodies at one year (6). The reason for this low rate of long-term humoral immunity was not clear, and a possible role for spike-specific or RBD-specific CD4 T cell responses was not studied (6). An earlier study had compared RBD-specific IgG levels, to the levels of CD4 responses to all viral antigens, but did not demonstrate a direct relationship between them (7), despite finding greater than 100-fold ranges in the individual levels of both neutralizing

antibody titres and CD4 T cell responses. Therefore, a better understanding is still required for the possible role of CD4 T cell responses in determining the initial level of neutralizing antibody titres in convalescent patients, and whether long-term memory CD4 T cells are important in regulating the observed variability of longevity of humoral immunity, that was reported by Xiang and colleagues (6).

A recent study of the immune response to the mRNA COVID-19 vaccine in SARS-CoV-2 naïve and recovered individuals showed a rapidly induced CD4 T cell response when compared to the gradually developing CD8 T cell response (8). Similarly, when we studied the immune response to vaccinia virus inoculation, highly activated antigen-specific CD4 T cells were often more expanded than corresponding CD8 T cells in blood early in the response (9, 10). Antigen-specific CD4 cytotoxic T lymphocytes (CTL) peaked at day 14, while neutralizing antibodies, and memory CD4 T cells that proliferated *in vitro* in response to vaccinia antigen appeared later at day 21 (9, 10). The early generation of CD127 (IL-7 receptor alpha chain)-expressing, IL-2-producing, proliferative memory CD4 T cells specific for vaccinia virus is most likely crucial to the long-term protection associated with immunity to smallpox (11). Such T cell proliferation in response to re-exposure to viral antigens is believed to be critical to allow more rapid response to re-infection, after the immune system had returned to homeostasis following contraction of the initial response to the acute infection [reviewed in (12)]. Overall, *in vitro* proliferation of PBMC in response to antigens derived from pathogens is highly correlated with effective immunity (13), due to rapid memory recall response.

A number of studies early in the pandemic identified SARS-CoV-2 specific CD4 T cells in COVID-19 patients (14-18). However, longer term studies showed a consistent average decline of memory CD4 T cells over time with a decrease until 60 days after the acute phase and maintained over 10 months with a central memory phenotype post 6 month (7, 19). Most of

these studies have used upregulation of markers of activation on antigen-specific CD4 T cells, similar to the original OX40 assay (20). In contrast there is very limited data on proliferative memory SARS-CoV-2-specific CD4 T cells (19, 21).

While CD4 T cell responses are important for antiviral humoral immunity, CD8 T cells are still believed to be important in cell-mediated immunity to respiratory viruses (22). Studies investigating the properties of SARS-CoV-2 reactive CD8 T cells report a high diversity of functional SARS-CoV-2 specific CD8 T cells (23–25), with cross-reactivity to seasonal coronavirus antigens (26). This indicates that CD8 T cells could be important in viral clearance in individuals that lack neutralizing antibodies (27, 28), although they often display an exhausted phenotype (23, 24).

In the current study we systematically studied SARS-CoV-2-specific proliferation of CD4 and CD8 T cells in recovered COVID-19 patients to better define the extent of their long-term memory cells. Importantly, RBD-specific proliferative memory CD4 T cells were closely associated with levels of neutralizing antibodies in recovered patients and in vaccinees. Furthermore, single cell RNAseq/TCRseq was used to study the function of individual SARS-CoV-2 reactive CD4 T cells from subjects with high antibody titres.

## 2 Materials and methods

### 2.1 ADAPT cohort

The ADAPT study is a prospective cohort study of post-COVID-19 recovery established in April 2020 (29), with ongoing recruitment (147 participants with confirmed SARS-CoV-2 infection had been enrolled at the time of writing). The majority were recruited following testing in community-based clinics run by St Vincent's Hospital Sydney, with some patients also enrolled with confirmed infection at external sites. Initial study follow-up was planned for 12 months post-COVID-19, and subsequently extended to 2 years. Extensive clinical data was systematically collected, including classification of disease severity, as previously described (29) and a prospective biorepository established, as previously described (30). Subjects classified with mild COVID-19 were those managed in the community with minor, largely upper respiratory tract viral symptoms, including pharyngitis, rhinorrhea, headache, and anosmia/ageusia. Subjects with moderate COVID-19 were managed in the community with fever/chills and one of the following organ-localizing symptoms, or at least two of the following organ-localizing symptoms: cough, hemoptysis, shortness of breath, chest pain, nausea/vomiting, diarrhea, altered consciousness/confusion. Subjects with severe COVID-19 were those who required inpatient care (wards or intensive care unit), as previously described (29). Laboratory testing for SARS-CoV-2 was performed using nucleic acid detection from

respiratory specimens with the EasyScreen™ SARS-CoV-2 Detection kit (Genetic Signatures, Sydney, Australia). Enrolment visits were performed at median 76 (IQR 64–93) days after initial infection (3-months) and 8-month assessments were performed at median 232 (IQR 226–253) days after initial infection. Serum and PBMCs were collected from ADAPT study participants following vaccination with either 2 doses of BNT162b2 (Pfizer) or ChAdOx1 (AstraZeneca).

The demographics of the ADAPT study participants in this report (first wave patients, recruited prior to October, 2020) are shown in **Supplementary Table 1**. Unexposed healthy adult donors ( $n=13$ ; 45% male; median age 46) were recruited through St Vincent's Hospital, were anti-spike antibody negative, and tested prior to vaccination.

### 2.2 Ethics

The ADAPT study was approved by the St Vincent's Hospital Human Research Ethics Committee (2020/ETH00964) and is a registered trial (ACTRN12620000554965). ADAPT-C sub study was approved by the same committee (2020/ETH01429). All data were stored using REDCap electronic data capture tools. Unexposed healthy adult donors were recruited through St Vincent's Hospital which was approved by St Vincent's Hospital Human Research Ethics Committee (HREC/13/SVH/145 and HREC/10/SVH/130). All participants gave written informed consent.

### 2.3 Antigens

Recombinant SARS-CoV-2 RBD polypeptide was produced using DNA encoding a His-tagged 200 amino acid region, for residues 319 to 541 of SARS-CoV-2 S protein, as previously described (31), corresponding to the following amino acid sequence: RV QPTESIVRFP NITNLCPFGE VFNATRFASV YAWNKRKRN CVADYSVLYN SASPSTFKCY GVSPTKLNLD CFTNVYADSF VIRGDEVQRQI APGQTGKIAD YNYKLPDDFT GCVIAWNSNN LDSKVGGNYN YLYRFRKSN LKPFERDIST EIYQAGSTPC NGVEGFNCYF PLQSYGFQPT NGVGYQPYRV VVLSFELLHA PATVCGPKKS TNLVKNKCVN FG SHHHHHH, which was cloned into pCEP4 vector (Thermo Fisher) and expressed transiently in Expi293 cells (Thermo Fisher) using the Expifectamine transfection kit (Thermo Fisher). After 7 days of expression, the culture supernatant was filtered, dialysed against PBS and the protein purified using the His-tag and Talon resin (Thermo Fisher), as previously described (31).

Recombinant trimeric SARS-CoV-2 spike protein was expressed from a plasmid encoding the spike protein with C-terminal trimerization domain and His tag which was a gift from the Kramer lab (BEI Resources, NIAID, NIH). The plasmid was transfected into Expi293 cells and protein expressed for 3

days at 37°C, 5% CO<sub>2</sub>. The protein was purified using the His tag as for the RBD purification. The protein was further purified on a Superose 6 gel filtration column (GE Healthcare) using an AKTA Pure FPLC instrument (GE Healthcare) to isolate the trimeric protein and remove S2 pre-fusion protein, as previously described (31). Pools of 15-mer peptides corresponding to the sequence of SARS-CoV-2 spike protein were purchased from Genscript (Hong Kong) and are listed in [Supplementary Table 2](#). His-tagged purified recombinant spike proteins from human coronavirus strains 229E, NL63 and OC43 were purchased from SinoBiologicals US (Wayne, PA, USA). Anti-CD3/anti-CD28/anti-CD2 polyclonal T cell activator was purchased from StemCell Technologies (Vancouver, Canada). Purified Influenza A (A/Sydney/5/97) was a gift from Alan Hampson, CSL, as previously described (20).

## 2.4 CD25/OX40 assay

Peripheral blood mononuclear cells (PBMC) were isolated from EDTA anti-coagulated blood within 4 hr of venepuncture, as previously described (10). Antigen-specific CD4 T cells responding to recall antigens, simultaneously up-regulating CD25 and CD134 (OX40), were measured in cultures of 300,000 PBMC in 200 µl/well of a 96-well plate, in Iscove's Modified Dulbecco's Medium (IMDM; ThermoFisher, Waltham, MA, USA) containing 10% human serum (kind gift, Dr Wayne Dyer, Australian Red Cross Lifeblood, Sydney, Australia), which were incubated for 44–48 hr, in a 5% CO<sub>2</sub> humidified incubator, as previously described (20). Separate cultures were incubated with individual SARS-CoV-2 antigens as indicated. All experiments additionally included: (i) a culture medium only, negative control well; (ii) anti-CD3/anti-CD28/anti-CD2 T cell activator (1/200 dilution), polyclonal positive control well; and (iii) influenza virus (1/200 dilution), antigen positive control well. PBMC from the respective cultures were stained with CD3-PerCP-Cy5.5, CD4-FITC, CD25-APC, and CD134-PE (BD Biosciences, San Jose, CA, USA) and run on a 5-laser Fortessa X20 (BD Biosciences) as previously described (32). Antigen-specific CD4 T cells were gated and expressed as CD25+CD134+ % of CD4+ CD3+ T cells as previously described (20). Cultures were classified as positive for antigen-specific CD4 T cells if the CD25+CD134+ % of CD4+ CD3+ T cells was  $\geq 0.2\%$  (33).

## 2.5 Cell Trace Violet proliferation assays

PBMC were resuspended at a concentration of  $10 \times 10^6$ /ml in PBS and incubated with Cell Trace Violet (CTV) dye (ThermoFisher) at 5 µM for 20 min at RT, according to the manufacturer's directions. Cells were washed once with 5x volume of IMDM/10% human serum and resuspended for cultures of 300,000 PBMC in 200 µl/well of a 96-well plate and

incubated for 7 days in a 5% CO<sub>2</sub> incubator. Different wells contained different antigens as indicated. All experiments also included: (i) culture medium only negative control well; (ii) anti-CD3/anti-CD28/anti-CD2 T cell activator (1/200 dilution) polyclonal positive control well; and (iii) influenza virus (1/200 dilution) antigen positive control well. After 7 days, cells from the respective cultures were stained with CD3-PerCP-Cy5.5, CD4-FITC, CD8-APC-H7 and CD25-APC (BD Biosciences), and analysed on a 5-laser Fortessa X20 (32) and antigen-specific CD4 T cells gated as CD3+CD4+CD25<sup>high</sup>CTV<sup>dim</sup> as previously described (34). Cultures were classified as positive for antigen-specific CD4 T cells if the CD25<sup>high</sup>CTV<sup>dim</sup> % of CD4+ CD3+ T cells was  $\geq 1\%$ .

## 2.6 Intracellular analysis of transcription factors

Expanded CD25<sup>high</sup>CTV<sup>dim</sup> antigen-specific CD4+ CD3+ T cells at the end of a 5 day incubation period were analysed for expression of intracellular markers including transcription factors, cytotoxic effector molecules and CTLA-4 using Transcription Buffer permeabilization reagents (BD Biosciences), according to the manufacturer's directions. The monoclonal antibodies used were: Tbet-BV711 (BioLegend); RORγT-PE and CTLA-4-PECy5 (BD Biosciences); Eomes-PE-Cy7, Bcl6-PerCP-eFluor 701 and Foxp3-AF700 (eBiosciences, ThermoFisher). Following intracellular staining, cells were resuspended in 1% paraformaldehyde/PBS and analysed on the 5-laser Fortessa X20.

## 2.7 Ex vivo phenotyping and combined CD4/CD8 T cell activation assay

Cryopreserved PBMCs were thawed using RPMI medium containing L-glutamine and 10% FCS (ThermoFisher Scientific, USA) supplemented with Penicillin/Streptomycin (Sigma-Aldrich, USW), and subsequently stained with monoclonal antibodies (mAb) binding to extracellular markers. Extracellular panel included: Live/Dead dye Near InfraRed, CXCR5 (MU5UBEE), CD38 (HIT2) (ThermoFisher Scientific, USA); CD3 (UCHT1), CD8 (HIL-72021), PD-1 (EH12.1), TIM-3 (TD3), CD27 (L128), CD45RA (HI100), IgD (IA6-2), CD25 (2A3), and CD19 (HIB19) (BioLegend, USA); CD4 (OKT4), CD127 (A019D5), HLA-DR (L234), GRP56 (191B8), CCR7 (G043H7) and CD57 (QA17A04) (BD Biosciences, USA). FACS Perm Buffer II (BD Biosciences) was used for intracellular staining of granzyme B (GB11, BD Biosciences). FACS staining of 48hr activated PBMCs was performed as described previously, but with the addition of CD137 (4B4-1) to the cultures at 24hrs. Final concentration of 10µg/mL of SARS-CoV-2 peptide pools (Genscript) were used, 1 µg/mL of

Influvac tetra influenza vaccine (Mylan Health, Sydney, Australia) was used as a control antigen and staphylococcal enterotoxin B (SEB; 1 µg/ml) was used as a positive control (ThermoFisher Scientific). *In vitro* activation mAb panel included: CD3 (UCHT1), CD4 (RPA-T4), CD8 (RPA-T8), CD39 (A1), CD69 (FN50) all BioLegend, CD25 (2A3), CD134 (L106)- BD Biosciences. Samples were acquired on the Aurora CS spectral flow cytometer (Cytex Biosciences, USA) using the Spectroflo software. Prior to each run, all samples were fixed in 0.5% paraformaldehyde. Data analysis was performed using FlowJo version 10.7.1 (BD Biosciences).

## 2.8 Anti-spike and anti-nucleocapsid diagnostic serology

Antibodies to SARS-CoV-2 spike in serum samples from ADAPT subjects were measured using the LIAISON<sup>®</sup> SARS-CoV-2 S1/S2 IgG diagnostic assay (Diasorin, Saluggia, Italy). This method quantitatively detects IgG anti-S1 and anti-S2 specific antibodies by indirect chemiluminescence immunoassay, using recombinant S1 and S2 antigens. Antibodies to SARS-CoV-2 spike were also measured using the Euroimmun diagnostic ELISA for IgG anti-S1 (Luebeck, Germany).

Antibodies to SARS-CoV-2 Nucleocapsid were measured using the Abbott Architect diagnostic chemiluminescent immunoassay (Abbott Park, IL, USA), and the Euroimmun NCP diagnostic ELISA assay (Euroimmun). All assays were done according to the manufacturers' directions.

## 2.9 Flow cytometry based IgG/IgM serology

The assay to detect patient serum antibodies against SARS-CoV-2 antigens using flow cytometry has been previously described in detail (35). Briefly, HEK293 cells were transfected to transiently express SARS-CoV-2 full-length Spike (Wuhan-1 D614), Membrane and Envelope proteins. Diluted patient serum was added to the cells, followed by adding AlexaFluor 647-conjugated anti-human IgG (H+L) (Thermo Fisher Scientific) or anti-human IgM (A21249, Thermo Fisher Scientific). The LSRII flow cytometer (BD Biosciences, USA) was used to acquire the cells and patients were confirmed SARS-CoV-2 antibody positive if, in at least two of three quality-controlled experiments, their median fluorescence intensity ( $\Delta\text{MFI} = \text{MFI transfected cells} - \text{MFI untransfected cells}$ ) was above the positive threshold (mean  $\Delta\text{MFI} + 4\text{SD}$  of 24 pre-pandemic controls). Data were analysed using FlowJo 10.4.1 (BD Biosciences), Excel (Microsoft, USA), and GraphPad Prism (GraphPad Software, USA).

## 2.10 Live virus neutralization assay

HEK293T cells were transduced with lentiviral particles to stably express human ACE2 and TMPRSS2. Briefly, the lentiviral expression vectors pRRLsinPPT.CMV.GFP.WPRE (36) and pLVX-IRES-ZsGreen (Clontech) were used to clone the ORFs for hACE2 (#1786, Addgene, Watertown, MA, USA) and hTMPRSS2a (#53887, synthetic gene fragment; Addgene), respectively. Lentiviral particles for transduction, to express the above proteins, were produced by co-transfecting the second generation lentiviral packaging constructs psPAX2 (courtesy of Dr Didier Trono through NIH AIDS repository) and VSVG plasmid pMD2.G (#2259; Addgene) and the expression plasmids individually in HEK293T cells (Life Technologies) using polyethyleneimine, as previously described (37). To generate the HEK293/ACE2/TMPRSS2a cells, two successive rounds of lentiviral transductions were performed; the highly permissive clone, HekAT24 was identified by clonal selection and then used to carry out the SARS-CoV-2 neutralisation assay as previously described (37).

To perform the assay, HekAT24 cells were trypsinized and while in suspension stained with Hoechst-33342 dye (5% v/v) (NucBlue, Invitrogen) and then seeded in a 384-well plate (Corning #CLS3985) at 16,000 cells per well in 40µL of DMEM-5% FCS. Patient plasma samples were mixed at two-fold dilutions with an equal volume of SARS-CoV-2 virus solution ( $4 \times 10^3$  TCID<sub>50</sub>/ml). Following incubation at 37°C for 1 hour, 40µL were transferred in duplicate to the cells (final MOI = 0.05). The following variants of concern were included as viral variants: Beta (B.1.351), Gamma (P.1), Delta (B.1.617), as well as control virus from the same clade with matching 'D614G' background (B.1.319). Following 24 hours of incubation, entire wells were imaged by high-content fluorescence microscopy and an automated image analysis software obtained the cell counts. The following formula was used to calculate the percentage of virus neutralisation:  $\%N = (D - (1 - Q)) \times 100/D$ , where Q = nuclei count normalized to mock controls and D = 1 - Q for average of infection controls as previously described (37). Neutralisation activity, NT<sub>50</sub> was defined as the serum dilution that led to 50% neutralization of infection.

## 2.11 Dimensional reduction and clustering analysis

FCS3.0 files were compensated manually using acquisition-defined matrix as a guide, and gating strategy was based on unstained or endogenous controls. Live singlets were gated from proliferated CD25+CTV- CD4+, or CD8+, respectively, CD3+ T cells using FlowJo v.10.7.2, samples were decoded and statistical analysis between groups and unsupervised analysis was performed. For unsupervised analysis, the following FlowJo

plugins were used: DownSample (v.3), UMAP (v.0.2), Phenograph (v.3.0) and ClusterExplorer (v.1.5.9) (all FlowJo LLC). Equal number of events for each condition were taken from each grouped sample by down sampling. The two new FCS files corresponding to Ab high and Ab low were then concatenated for dimensionality reduction analysis using UMAP. UMAP was conducted using the following parameters for proliferated CD4 T cells: T-bet, Eomes, Granzyme B, Foxp3, ROR $\gamma$ t, and BCL-6; and for CD8<sup>+</sup> T cells: T-bet, Eomes, Granzyme B and CTLA-4. The Phenograph plugin was then used to determine clusters of phenotypically related cells. The same markers as TriMap and parameters  $k = 152$  and Run ID = auto was used for analysis. Finally, ClusterExplorer plugin was used to identify the phenotype of the clusters generated by Phenograph.

## 2.12 Single cell RNA-seq analysis of antigen-specific T cells

PBMC from 4 Ab high donors were cultured for 48 hr with NP, spike and RBD peptide pools, respectively (Supplementary Table 2), as for the OX40 assays (see above). A total of 14,053 SARS-COV-2 specific CD25+OX40<sup>+</sup> CD4 T cells from these cultures were purified using FACSAriaIII cell sorter (BD biosciences), as shown in Supplementary Figure 6A. Unstimulated purified CD45RO<sup>+</sup> ex vivo memory CD4 T cells were used as a comparator subset (Supplementary Figure 6B). Purity of sorted populations were >99%. Populations were individually stained with Total-Seq C hashtags (BioLegend), and single cell libraries were generated using the 5<sup>'</sup>v2 Gene expression and immune profiling kit (10x Genomics). Subsequent cDNA and TCR libraries were generated according to manufacturer's instructions. Generated libraries were sequenced on the NovaSeq S4 flow cell (Illumina) at Read 1 = 28, i7 index = 10, i5 index = 10 and Read 2 = 90 cycles according to manufacturer's instructions.

## 2.13 Transcriptomic analysis

### 2.13.1 Pre-processing of raw sequencing files

Single-cell sequencing data was aligned and quantified using Cell Ranger (10x Genomics) against the human reference genome (10x Genomics, July 7, 2020 release) with default parameters. Raw hashtag data was processed using CITE-Seq count algorithm (38). Cell conditions were demultiplexed using 'HTODemux' function implemented in Seurat (38). Filtering and quality control was performed using Seurat (39) on data containing 15,276 cells where 14,053 cells were retained satisfying thresholds of both <10% mitochondria content and number of genes between 300 and 5000. 'SCTransform' was used for normalization (40). Genes encoding BCR and TCR were

removed to improve cell clustering. Principal Component Analysis (PCA) dimensional reduction was performed on variable genes identified by 'VariableFeatures' function and cell clusters were visualised using Uniform Manifold Approximation and Projection (UMAP) clustering implemented in Seurat (39).

### 2.13.2 Annotation of cell identities and differential gene expression analysis

T cell sub-populations were manually annotated based on UMAP clustering and markers defined by 'FindAllMarkers' function in Seurat.

Raw counts from defined cell populations were normalised using scran/scater (41, 42) and differential gene expression analysis was performed using Limma voom (43).

## 2.14 TCR analysis of bulk proliferated cells

RNA was extracted from bulk proliferated cultures using RNAeasy micro kit (Qiagen) as per manufacturer's instructions. TCR high throughput RNA sequencing methods have been previously published in detail (44). Briefly, reverse transcription of RNA was performed using a modified SmartSeq2 protocol that incorporated a 10bp universal molecular identifiers (UMI) into cDNA molecules. The first round of PCR was performed using primers against adapter sequences incorporated during cDNA synthesis with 1x KAPA HiFi HotStart ReadyMix and 8.3 mM Fwd and Rev primer with the following conditions: 98°C for 3 min; [98°C for 20 s, 67°C for 15 s, 72°C for 6 min] x 10 cycles; 72°C for 5 min. Purified PCR products were used in a second PCR targeting the TCR $\beta$  chain under the following conditions: 98°C for 45 s; [98°C for 15 s, 60°C for 30 s, 72°C for 30 s] x 30 cycles; 72°C for 1 min. Purified PCR products were then barcoded using the Nextera Index kit to enable pooling of multiple samples and sequenced on an Illumina MiSeq at 300bp paired-end reads to a depth of ~0.5 million read pairs per sample. Primer sequences were as previously described (44).

## 2.15 Analysis of single cell and bulk TCR datasets

Bulk TCRB datasets for the proliferation assay were processed with the Presto package (version 0.7.0 2021.10.28) (45). Reads were filtered for a minimum quality score of 20 using FilterSeq. R2s were trimmed of the TRC primer using MaskPrimers requiring exact primer matches. MaskPrimers was also used to extract the 10 nucleotide UMIs from R1 and to trim to TSO sequences. Trimmed R1 and R2 were paired with PairSeq and consensus UMIs were defined with BuildConsensus. R1 and R2 were then merged with AssemblePairs and the dataset

was dereplicated to unique sequences and converted from fastq to fastq with CollapseSeq. Sequences with ambiguous bases (n) were discarded. Dereplicated fasta datasets were aligned against the IMGT human TCR reference directory [<https://www.imgt.org/vquest/refseqh.html>, downloaded 16-Jan-2020] using IgBLAST (46) via AssignGenes to generate AIRR formatted output.

To ensure consistent gene calling, TCR contigs from 10x's cellranger v2 were re-aligned to the IMGT human TCR reference set with AssignGenes from the Presto package. Change-o databases were generated with MakeDb and subset to TCRA and TCRB with ParseDb from the Change-o package (version 1.2.0 2021.10.29) (47).

TCR clonotypes were defined using the TCRV, TCRJ and CDR3 AA sequence. Clonotype information from 10x VDJ was integrated with the 10x scRNA-seq within the Seurat package (version 4.1.0) (48) in R [R Core Team (2020). R: A language and environment for statistical computing. R Foundation for Statistical Computing, Vienna, Austria. URL <https://www.R-project.org/>] using RStudio [RStudio Team (2021). RStudio: Integrated Development Environment for R. RStudio, PBC, Boston, MA URL <http://www.rstudio.com/>] based on shared cell barcodes. For the proliferation assay bulk sequencing, enrichment was calculated by comparing clonotype UMI counts in stimulation conditions versus baseline/unstimulated with a pseudocount of 1 for clonotypes that were absent from the baseline sampling. Proliferation assay data was merged with the 10x data based on shared TCRB clonotypes.

TCR repertoires were explored using the tidyverse package (49) to aggregate and summarise data. Diversity was calculated as Shannon's Entropy (50) as implemented by the entropart package (51). Repertoire features were visualised with ggven [<https://CRAN.R-project.org/package=ggven>], circos (52), ggpubr [<https://CRAN.R-project.org/package=ggpubr>] and ggsci [<https://CRAN.R-project.org/package=ggsci>].

To annotate previously reported SARS-CoV-2 specific T cells, TCRBs reported to bind SARS-CoV-2 epitopes were obtained from two public resources; immuneCODE MIRA (release 002.2) (53) and VDJdb (v2021-09-05) (54). TCRB clonotype labels were reformatted for consistency and clonotypes were annotated based on shared clonotype labels between the databases and dataset.

## 2.16 Statistical analysis

All column graphs are presented as medians with inter-quartile ranges. Mann-Whitney non-parametric test was used to compare unpaired groups and Pearson's correlation was used to analyse statistical relationships between continuous variables, employing Prism 9.0 software (GraphPad, La Jolla, CA, USA).

RStudio version 1.2.1335 was used to generate PCA graphs. *p* values <0.05 were considered significant (\*<0.05, \*\*<0.01, \*\*\*<0.001, and \*\*\*\*<0.0001).

## 3 Results

### 3.1 Proliferative RBD-specific CD4 T cells correlate with neutralising antibody titres

To assess memory CD4 T cell responses following SARS-CoV-2 infection, we screened 27 ADAPT subjects from the first wave (May-October, 2020; [Supplementary Table 1](#)) at 3 months post-infection using recombinant SARS-CoV-2 RBD protein, and using influenza lysate as a control antigen. We utilised our CD25/OX40 (20) assay to assess antigen-specificity of CD4 T cells and found overall a 13.5-fold higher response to RBD in ADAPT subjects (median 0.46%) at 3 months compared to unexposed controls (n=13; median 0.034%, *p*<0.0001) ([Figures 1A, B](#)). However, 7/27 ADAPT subjects were negative (<0.2%) for a response to RBD ([Figure 1B](#)). All unexposed controls and ADAPT subjects had positive flu specific responses (medians 1.51% and 1.62%, respectively).

Having seen initial OX40 responses to RBD, for subsequent patients, we used the 7-day PBMC proliferation assay with cell trace violet dye (CTV; [Supplementary Figure 2](#)) to confirm the presence of memory CD4 T cells. There was no CD4 T cell proliferation response to RBD (< 1% of CD4 T cells) in PBMC from unexposed controls (n=6), while the ADAPT subjects (n=13) had an overall median proliferation of 11.1%, *p*<0.01. Again the results were heterogeneous with 6 of the 13 ADAPT subjects tested having < 1% CD4 T cell proliferation in response to RBD, similar to the unexposed controls in this assay ([Figure 1C](#)). Proliferation responses to Flu lysate, by both control and patient PBMC, were all positive, similar to the OX40 results, and generally larger than the responses to SARS-CoV-2 RBD ([Figure 1C](#)). There was a highly significant positive correlation between CD25+ OX40+ CD4 T cell responses to RBD and CD4 T cell proliferation responses to RBD (pearson's rho=0.89, *p*<0.0001) ([Figure 1D](#)), as we have previously reported for a variety of other recall antigens (20).

When we compared the levels of anti-spike IgG, measured in the ADAPT subjects' 3-month follow-up serum using the diagnostic DiaSorin Liaison assay, the proliferation of RBD-specific CD4 T cells positively correlated with anti-spike IgG levels (rho=0.52, *p*<0.01; [Figure 1E](#)). We also used a flow-based assay (35) to measure spike (Wuhan-1 D614)-specific IgG and IgM in patients' serum samples, which gives scores of 0-3 for each antibody isotype (where 3 is highest). When the IgG and IgM scores were combined, the patients with RBD-specific CD4 T cell responses had significantly higher antibody levels (median

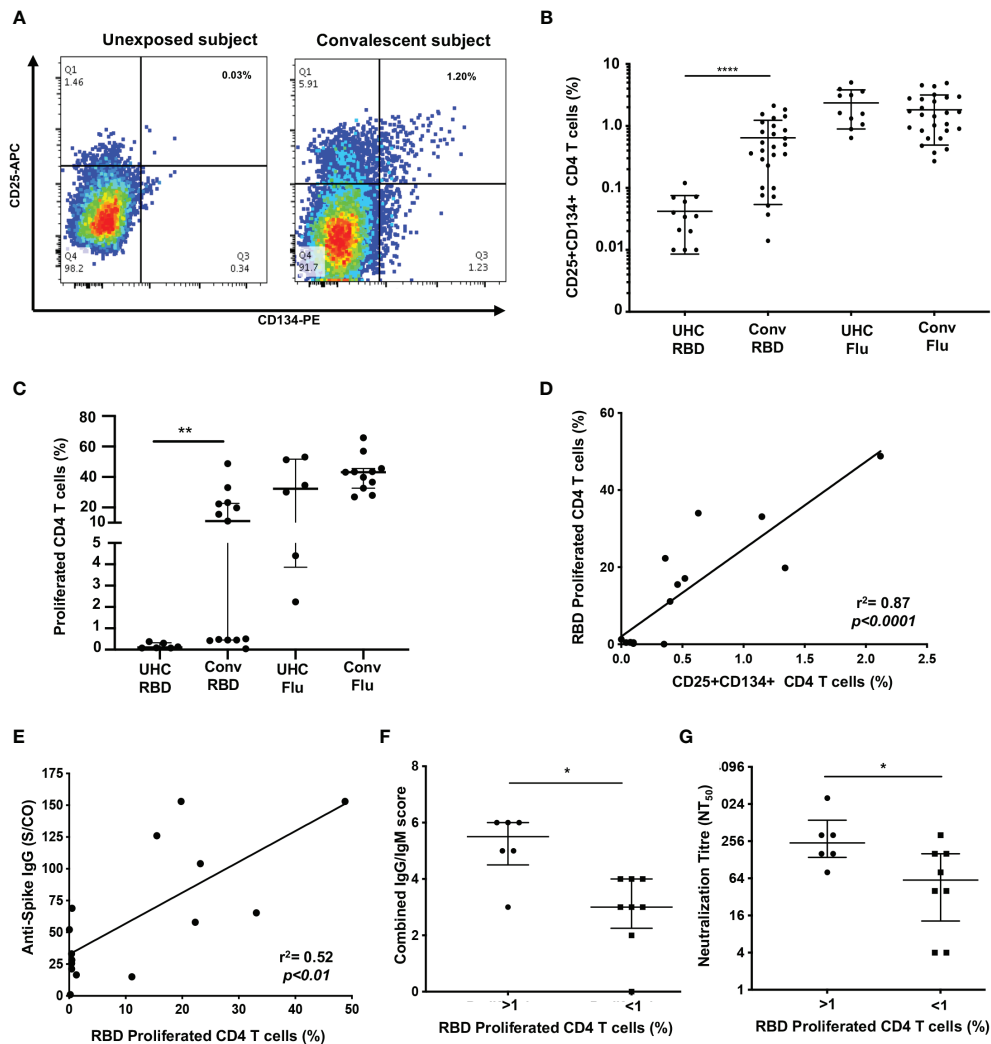


FIGURE 1

Proliferation of SARS-CoV-2 reactive CD4+ T cells correlate with antibodies. (A) Representative dot plots of CD25+CD134+ co-expression on RBD-specific CD4+ T cells. (B) Frequency of RBD reactive CD4+ T cells in convalescent subjects (conv) compared to unexposed healthy controls (UHC). (C) Percentage of proliferating CD4+ T cells stimulated with RBD or Flu antigen. (D) Positive correlation between recall CD25+CD134+ CD4 response and 7 days of proliferation. (E) Correlation between spike IgG levels and RBD specific proliferation of CD4+ T cells. (F) Convalescent subjects with proliferated CD4+ T cells (>1%) are Ab high vs subjects without proliferation (<1%) are Ab low, based on combined IgG/IgM score. (G) Subjects with proliferated CD4+ T cells (>1%) have significantly higher neutralizing Ab titres (NT<sub>50</sub>) vs subjects without proliferation (<1%). Data shown as medians with interquartile ranges. Two-tailed p values <0.05 were considered significant (\*<0.05, \*\*<0.01, \*\*\*<0.001, \*\*\*\*<0.0001). Mann-Whitney T tests were used for unpaired groups and Pearson's rho was used for correlations.

score of 5.5) than patients with negative proliferative responses to RBD (median score of 3,  $p < 0.05$ ) (Figure 1F).

Finally, live virus neutralization assays were performed with the ADAPT patients' sera, measured as an end-point titre (35). The patients with RBD-specific CD4 T cell responses had significantly higher neutralization titres (NT<sub>50</sub>, median 256) than patients with negative proliferation results (median 64,  $p < 0.05$ ) (Figure 1G). Collectively these data demonstrate a heterogeneous memory immune response observed during natural infection with SARS-CoV-2.

### 3.2 Antibody high versus antibody low subject groups

In order to confirm the association of RBD-specific CD4 T cell responses with higher antibody levels, cryopreserved PBMC and serum samples were studied from an additional 24 ADAPT subjects, separated into two representative groups of 12 subjects each, with known high and low SARS-CoV-2 neutralisation titres, respectively, at month 3 (Supplementary Table 1). The selected antibody high (Ab high) subject group had



neutralisation titres  $NT_{50} \geq 80$ , whereas the antibody low (Ab low) group had neutralization titres  $NT_{50} \leq 40$  (Figure 2A). Neutralisation titres in the Ab high group gradually decreased over time with a median of 320 at 3-month, 240 at 4-month and 120 at 8-month timepoints (Figure 2B). Furthermore, the breadth of neutralizing antibodies to variants of concern was significantly greater in Ab high group at 3-months (Figure 2C), but also then decreased at 8-months (Figure 2D).

### 3.3 Reduced RBD-specific CD4 T cell responses in individuals with low antibody levels

We also widened our analysis of T cell responses to other SARS-CoV-2 antigens, using peptide pools (Supplementary Table 2), that also allowed us to adapt our CD25/OX40 CD4 assay to include the detection of antigen-specific CD8 T cells by

adding the co-expression of CD69 and CD137 (4-1BB) surface markers (55).

RBD-specific CD4 T cells were mostly undetectable in the Ab low group [median 0.12% (3-month) and 0.1% (8-month)], such that the fold difference in RBD-specific CD4 T cell responses between the 2 subject groups was 50-fold at month 3 ( $p < 0.001$ ), down to 15-fold at 8 months ( $p < 0.01$ ; Figure 3A).

There were also significantly higher CD4 T cell responses to the spike peptide pool in the Ab high subject group compared to the Ab low subject group (Figure 3A), although not as marked as for RBD (above), with a 5.3-fold higher spike-specific response at the 3-month time-point ( $p < 0.01$ ), which was still 3.9-fold higher at 8 months ( $p < 0.01$ ; Figure 3A).

Nucleocapsid protein (NP)-specific CD4 T cell responses were not significantly different between the 2 groups at 3-months, but there was a 15-fold higher frequency in the Ab high subject group compared to the Ab low subject group at 8-months ( $p < 0.01$ ).

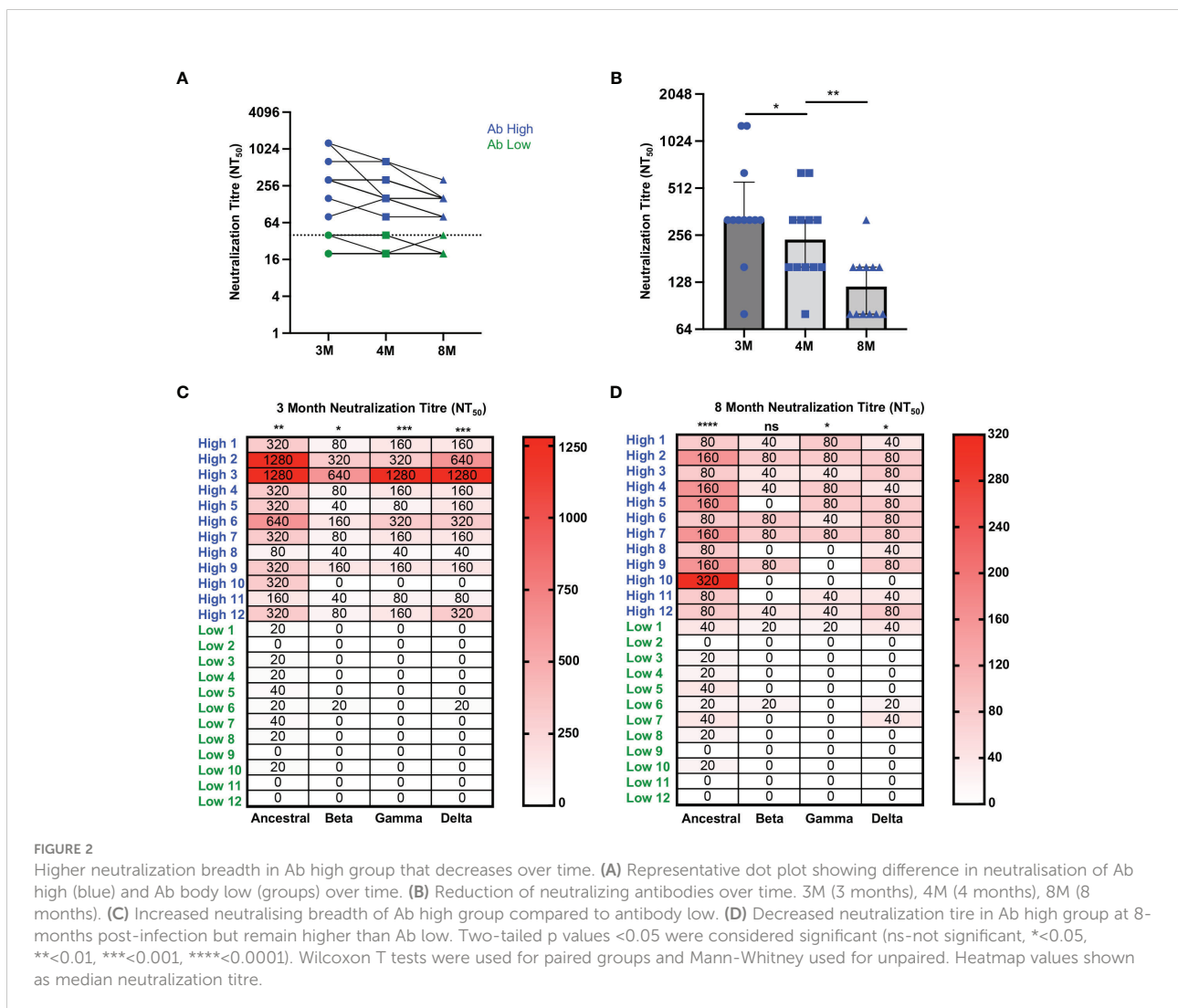


FIGURE 2

Higher neutralization breadth in Ab high group that decreases over time. (A) Representative dot plot showing difference in neutralisation of Ab high (blue) and Ab body low (groups) over time. (B) Reduction of neutralizing antibodies over time. 3M (3 months), 4M (4 months), 8M (8 months). (C) Increased neutralising breadth of Ab high group compared to antibody low. (D) Decreased neutralization titre in Ab high group at 8-months post-infection but remain higher than Ab low. Two-tailed p values  $< 0.05$  were considered significant (ns-not significant,  $* < 0.05$ ,  $** < 0.01$ ,  $*** < 0.001$ ,  $**** < 0.0001$ ). Wilcoxon T tests were used for paired groups and Mann-Whitney used for unpaired. Heatmap values shown as median neutralization titre.

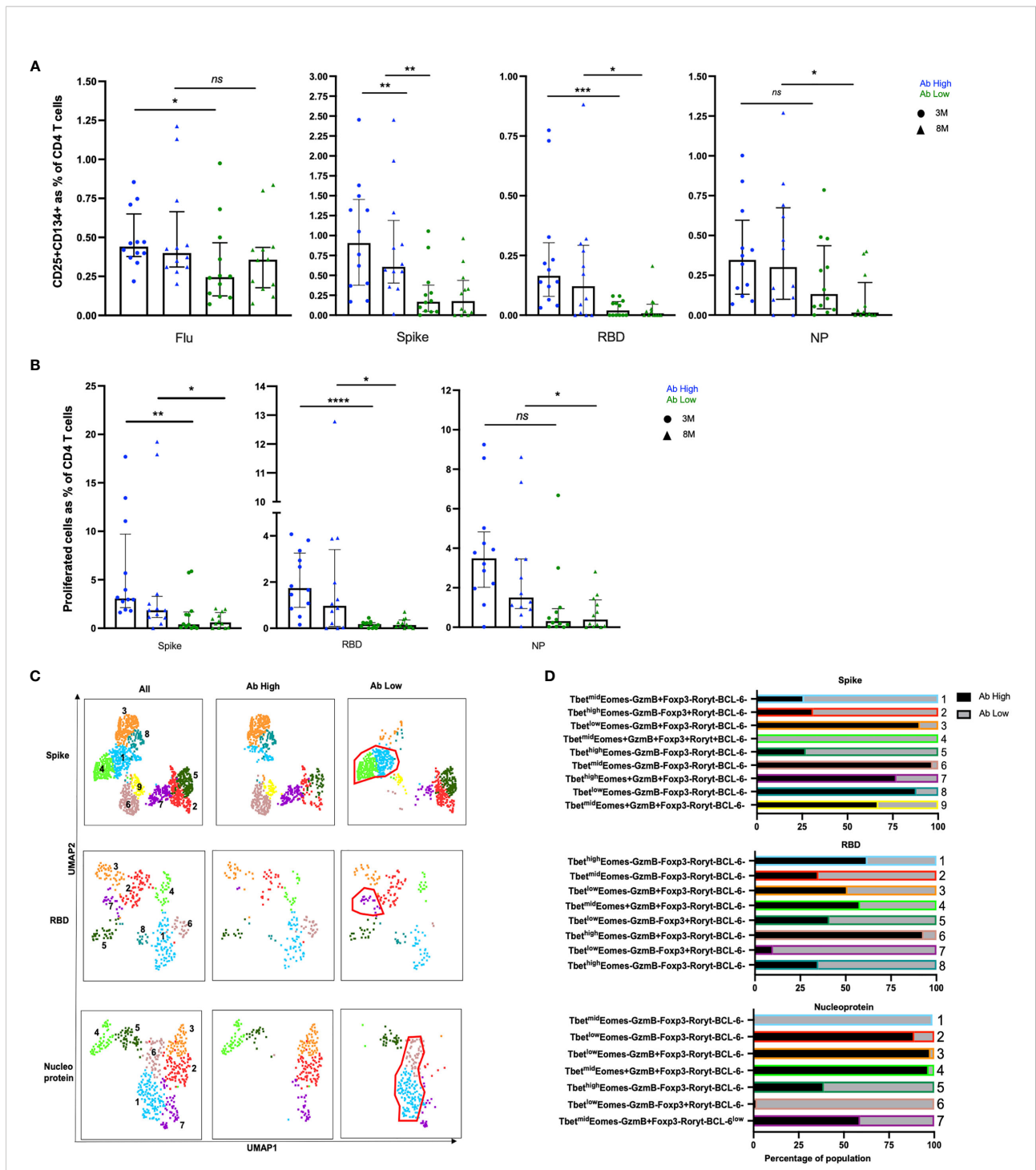


FIGURE 3

Higher frequencies of RBD-specific CD4+ T cells in Ab high group. (A) CD4 responses to influenza, spike, RBD and nucleoprotein (NP) at 3M and 8M post- infection. (B) Higher frequency of SARS-CoV-2 proliferative CD4 T cells in Ab high group compared to Ab low at 3M and 8M. (medians with interquartile ranges). (C) Representative UMAP of proliferated CD4 T cells: concatenated, ab high; and ab low. Red gates are regulatory-like cells present in Ab low subjects. (D) Regulatory-like Foxp3+ cells are higher in Ab low subjects (grey columns) compared with higher effector cells in Ab high subjects (black columns). The colour and number of horizontal bar graphs match with UMAP clusters. Two-tailed p values <0.05 were considered significant (ns-not significant, \*<0.05, \*\*<0.01, \*\*\*<0.001, \*\*\*\*<0.0001). Mann-Whitney T test used for unpaired samples.

No difference between the 2 groups was observed in the proportion of antigen-specific CD4 T cells that had a CD39+ Treg phenotype (56) (Supplementary Figure 3).

In addition, we also measured proliferation of CD4 T cells following peptide stimulation and found that there was significantly higher proliferating SARS-CoV-2-reactive CD4 T cells in the Ab high group at both 3- and 8-month timepoints for all 3 peptide pools (Figure 3B). Also, we independently confirmed that the Ab high group had significantly higher antibodies to Spike and Nucleocapsid, using 2 commercially available diagnostic assays for each antigen, respectively (Supplementary Figure 4).

Intracellular phenotyping (Supplementary Figure 5) of spike-specific proliferated CD4 T cells from the Ab high group showed 3 relatively large clusters of Granzyme B+ cells (clusters #3, #7 and #9; Figures 3C, D, top row) and relatively few regulatory-like cells expressing Foxp3 (clusters #2 and #4; Figures 3C, D, top row). In contrast, proliferated CD4 T cells, in response to the spike peptide pool, from subjects in the Ab low group revealed the greatly increased presence of the 2 clusters of regulatory-like cells expressing Foxp3 (clusters #2 and #4, Figures 3C, D, top row), and greatly reduced Granzyme B+ cells (clusters #3, #7 and #9, Figures 3C, D, top row), compared to the proliferated CD4 T cells from subjects in the Ab high group.

Similarly, in RBD-specific proliferated CD4 T cells, the Ab high group had an increased presence of a Granzyme B+Foxp3-cluster (#6; Figures 3C, D middle rows) and less cells in Foxp3+ clusters (#5 and #7; Figures 3C, D middle rows). The opposite was seen in the much smaller proportions of proliferated cells from the Ab low group (Figures 3C, D middle rows).

Nucleoprotein-specific proliferated CD4 T cells also showed a very similar trend, with distinct Foxp3+ versus Granzyme B+ clusters between the Ab high and low groups (Figures 3C, D bottom rows).

In CD8 T cell specific responses, defined by upregulation of CD137 and CD69, no significant difference was observed between the antibody high or low groups, when stimulated with the 3 SARS-CoV-2 peptide pools or influenza (Figure 4A). However, in proliferation responses, the antibody high group had 4.2-fold higher proliferating NP peptide pool-specific CD8 T cells at 3 months ( $p < 0.01$ ) and 6.6-fold at 8 months ( $p < 0.05$ ), and a trend to higher spike-specific proliferation, compared to the antibody low group (Figure 4B). The much smaller proportions of proliferated CD8 T cells from Ab low subjects had clusters with much higher levels of expression of the inhibitory ligand CTLA-4, compared to proliferated CD8 T cells from Ab high subjects for all 3 peptide pools (Figures 4C, D).

### 3.4 B cell plasmablasts, with more CXCR5+ CD4 T cells, and T cell activation are associated with high antibody levels

We used 20-parameter flow cytometry to determine whether there were ex vivo phenotypic differences in the B and T cell subsets of Ab high and Ab low groups. Higher frequencies of B cell plasmablasts (CD19+IgD-CD27+CD38+) were found in the Ab high group (3.2-fold,  $p < 0.05$ ) at 3 months, but no difference was observed at 8 months (Figure 5A). When CD19+ B cells were divided into memory subsets, there was no difference at either time point for naïve (IgD+CD27-), non-switched memory (IgD+CD27+) or switched memory (IgD-CD27+) (Figure 5B). However, there was higher proportion of double negative (IgD-CD27-) cells in Ab low group at both 3- (1.7-fold,  $p < 0.05$ ) and 8-months (1.6-fold,  $p < 0.05$ ).

When surface markers of CD4 T cells were analysed there was significantly increased expression of CXCR5 in the Ab high group at both 3- and 8-month timepoints (2.9-fold,  $p < 0.05$  and 2.5-fold,  $p < 0.01$ , respectively) and co-expressed activation markers HLA-DR+CD38+ (3-fold,  $p < 0.01$  and 1.9-fold,  $p < 0.01$ , respectively), compared to the Ab low group (Figures 5C, D). Activated CD8 T cells were also increased at 3-months in Ab high subjects (2.3-fold,  $p < 0.05$ ) but not at 8-months (Figure 5E).

Within canonical CD4 T cell subsets, a higher frequency of effector memory cells (Tem; CD45RA-CCR7-) was evident in the Ab high group (1.7-fold,  $p < 0.05$  (3-months) and 1.6-fold,  $p < 0.05$  (8-months), compared to the Ab low group, but no difference was seen in naïve (CD45RA+CCR7+), central memory (Tcm; CD45RA-CCR7+) or memory revertant cells (Temra; CD45RA+CCR7-; Figure 5F). However, naïve (CD45RA+CCR7+) CD8 T cells were significantly higher in the Ab low group (1.8-fold,  $p < 0.05$ ), compared to the Ab high group, at both timepoints (Figure 5G).

To ascertain the association between the results of the T cell function assays and antibody levels, Spearman's correlation was performed utilising Benjamini-Hochberg method to correct for multiple comparisons. Positive correlations of antibody levels and neutralization titres were observed with: B cell plasmablasts; CXCR5+ CD4 T cells; CD4 and CD8 T cell activation; and spike- and RBD-specific CD4 T cell recall and proliferative responses. In contrast, DN B cells, naïve CD4 and spike-specific CD8 recall responses were all negatively correlated with antibodies (Figure 5H). These same parameters were able to separate Ab high and low groups using PCA (Figure 5I).

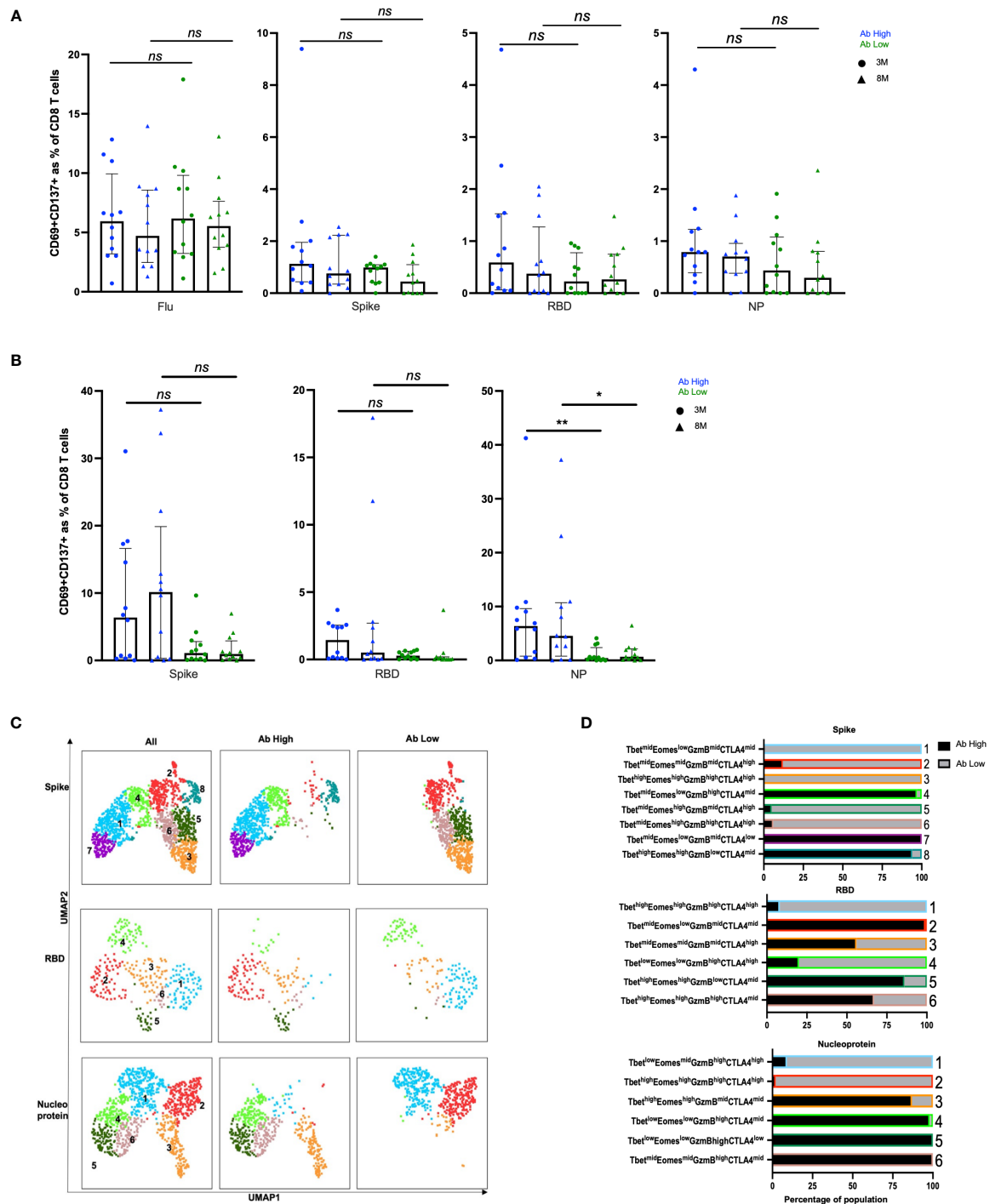


FIGURE 4

No difference in CD8 responses but presence of inhibitory receptors in Ab low subjects. (A) No difference between CD8 in Ab high and Ab low groups. (B) Higher frequency of NP proliferative CD8 T cells in Ab high group compared to Ab low. 3M (3 months) and 8M (8 months). Data shown as medians with interquartile ranges. (C) Representative UMAP of proliferated CD8 T cells; concatenated, ab high and ab low. (D) Presence of an inhibitory phenotype within cells of Ab low subjects. Colour and number of horizontal bar graphs match with UMAP clusters. Black columns (Ab high) and grey columns (Ab low). Two-tailed p values <0.05 were considered significant (\*<0.05, \*\*<0.01). Mann-Whitney T test used for unpaired samples. ns, not significant.

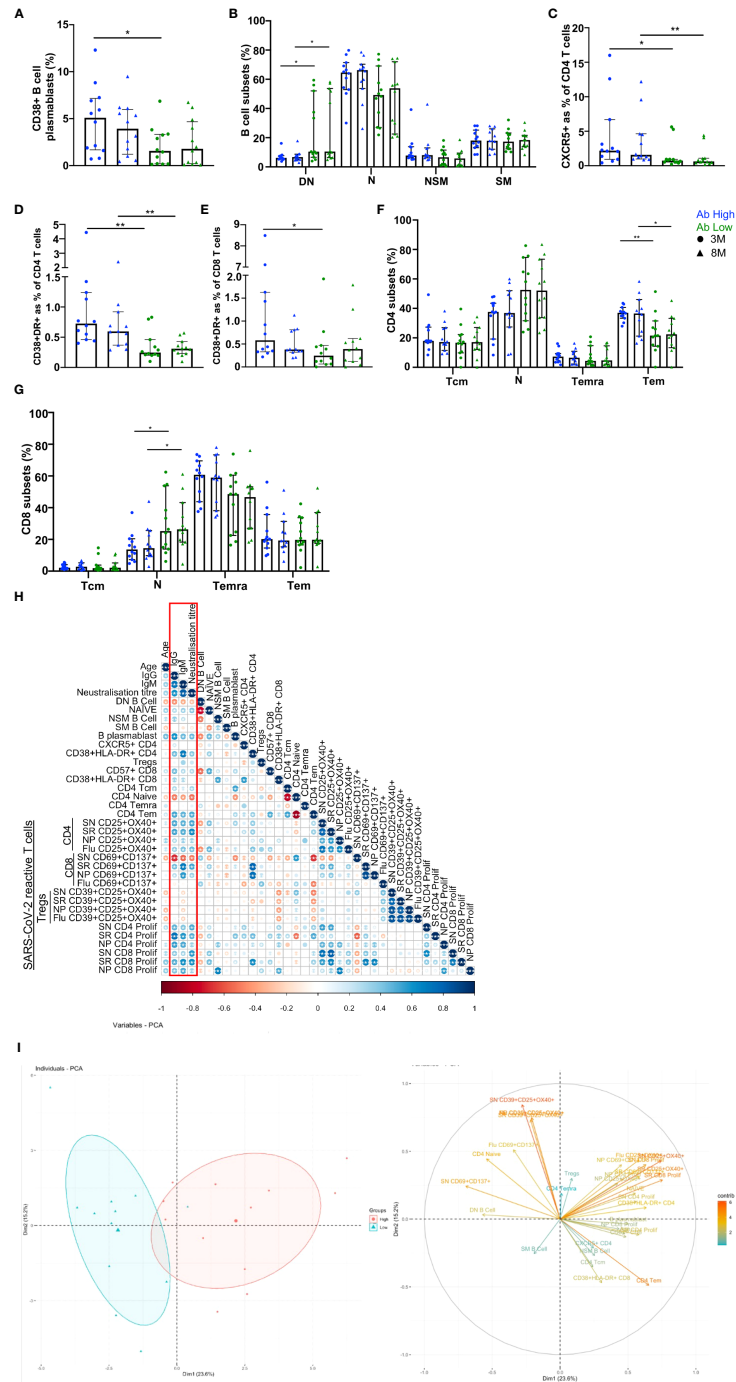


FIGURE 5

B and T cell parameters correlate with antibody response. **(A)** Higher CD38+ B cell plasmablasts in Ab high group. **(B)** Elevated double negative (DN, IgD-CD127-) B cells in Ab low group. Naïve (N, IgD+CD127-), non-switched memory (NSM, IgD+CD127+), switched memory (SM, IgD-CD127+) B cells. Higher CXCR5 expression on CD4s **(C)**, activation (CD38+HLA-DR+) on CD4 **(D)** and CD8 **(E)** and CD4 effector memory cells **(F)** in Ab High compared to Ab low group. Data shown as medians with interquartile ranges. **(G)** Higher naïve CD8+ T cells in Ab low group at both timepoints. SN (spike), SR (RBD), NP (nucleoprotein). Two-tailed p values <0.05 were considered significant (\*<0.05, \*\*<0.01, \*\*\*<0.001). Mann-Whitney T tests were used for unpaired groups. **(H)** B cell plasmablast, CXCR5+ CD4 T cells, activated CD4 and CD8 T cells, proliferative Spike and RBD-specific CD4 positively correlate with humoral response at 3 months post-infection (red box). **(I)** PCA clustering of Ab high and Ab low groups based on T and B cell parameters. Pearson's rho was used for correlations and adjusted p values shown with Benjamini-Hochberg correction used for multiple comparisons. Two-tailed p values <0.05 were considered significant (\*<0.05, \*\*<0.01, \*\*\*<0.001).

### 3.5 Single-cell RNAseq revealed heterogeneity and TCR diversity in SARS-CoV-2 reactive CD4 T cells

Our observations above showed that CD4 T cell recall responses to SARS-CoV-2 positively correlated with greater humoral responses, in particular RBD-specific responses in the Ab high subject group. To better understand these antigen-specific CD4 T cells, especially those specific for RBD, we cell sorted CD25+CD134+ CD4 T cells from 4 representative subjects from the Ab high group, following stimulation with peptide pools at 44hrs. Unstimulated purified memory CD4 T cells were used as the comparison population (Supplementary Figures 6A, B). Single-cell RNAseq was performed on a total of 14,053 cells comprising: (i) 9,039 *ex vivo* (unstimulated) memory cells; (ii) 2,026 NP-specific cells; (iii) 1,989 spike-specific cells; and (iv) 999 RBD-specific cells. Analysis of 10x transcriptomics was coupled with TCR $\alpha/\beta$  sequencing. We found heterogeneous subsets of CD4 T cells that were reactive to spike, RBD and NP; comprising transitional memory, central memory, Treg and cytotoxic subsets (Figures 6A, B). Enrichment of activated GTR+ Tregs (cluster 3) was particularly evident in the stimulated conditions (48.15%, 62.34% and 54.94% for NP- Spike- RBD-specific cells, respectively), compared to 3.08% for *ex vivo* memory cells (Figure 6C).

Analysis of TCR annotation was achieved on 11,824 single cells (84.14%). Diverse TCR responses resulted from all 3 stimulation conditions with similar Shannon Entropy score for the stimulation conditions compared to the unstimulated *ex vivo* (Supplementary Figure 7A) and diverse TCR $\alpha/\beta$  pairings for all four conditions (Supplementary Figure 7B). To examine if TCR $\alpha/\beta$  V gene was altered in the stimulated conditions compared to *ex vivo* memory, log odds-ratio analysis was performed with Bonferroni's correction. No difference was observed in the majority of TCR $\alpha/\beta$  V genes between *ex vivo* memory and stimulated conditions. However, there was increased usage of TCR $\alpha$  TRAV1-2/34/39 chains evident in NP-specific CD4 T cells compared to *ex vivo* memory (Figure 6D), while TRBV10-2 was the only TCR $\beta$  chain enriched in RBD-specific CD4 T cells (Figure 6E). With the exception of CD4 CTLs, where approximately half of the *ex vivo* unstimulated clones were re-sampled post-stimulation, generally antigen-specific clonotypes within the *ex vivo* unstimulated memory cell pool comprised only a tiny fraction of the antigen-specific clonotypes sampled following 2 days of antigen stimulation (Figure 6F). Clonotypes shared between unstimulated *ex vivo* CD4 memory and antigen specific pools rarely displayed altered cellular phenotypes following stimulation (Figure 6F).

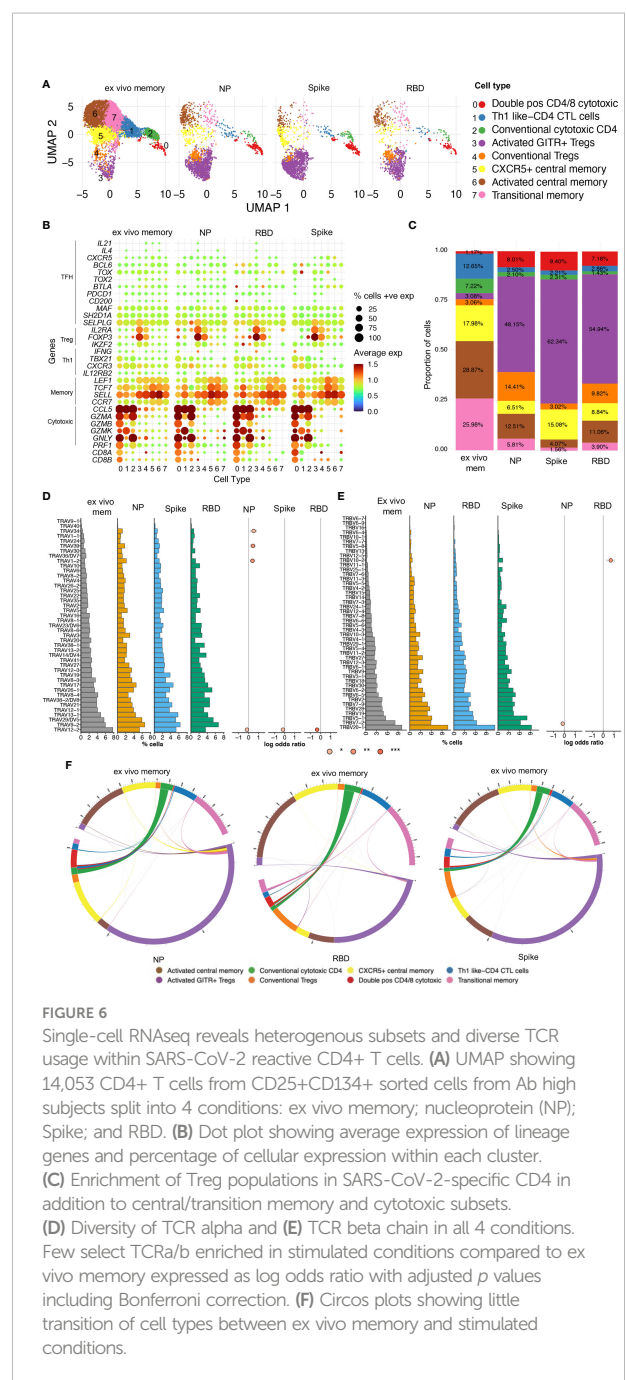


FIGURE 6

Single-cell RNAseq reveals heterogeneous subsets and diverse TCR usage within SARS-CoV-2 reactive CD4+ T cells. (A) UMAP showing 14,053 CD4+ T cells from CD25+CD134+ sorted cells from Ab high subjects split into 4 conditions: *ex vivo* memory; nucleoprotein (NP); Spike; and RBD. (B) Dot plot showing average expression of lineage genes and percentage of cellular expression within each cluster. (C) Enrichment of Treg populations in SARS-CoV-2-specific CD4 in addition to central/transition memory and cytotoxic subsets. (D) Diversity of TCR alpha and (E) TCR beta chain in all 4 conditions. Few select TCR $\alpha/\beta$  enriched in stimulated conditions compared to *ex vivo* memory expressed as log odds ratio with adjusted *p* values including Bonferroni correction. (F) Circos plots showing little transition of cell types between *ex vivo* memory and stimulated conditions.

### 3.6 Proliferative CD4 T cell clonotypes are enriched within cytotoxic and Treg subsets

To examine the clonal diversity of proliferative CD4 T cell subsets and confirm the single cell RNAseq clonotype data, we performed bulk TCR sequencing on T cells proliferating in response to NP, spike and RBD, compared to an unstimulated control, from

the same 4 patients as for the 10X transcriptomics. The TCR clonotypes found to be enriched by proliferation in the stimulated conditions compared to unstimulated were then matched to the same clonotype previously identified *via* 10X transcriptomics and overlaid on the same UMAP (Figure 7A).

10% of clonotypes were shared between the single cell RNAseq analysis and the proliferation assay TCR analysis. Enriched proliferative clonotypes identified in the SARS-CoV-2 antigen-stimulated cultures were most frequent in transcriptomic clusters comprising: (i) conventional Granzyme B+ CD4 CTL (cluster 2;

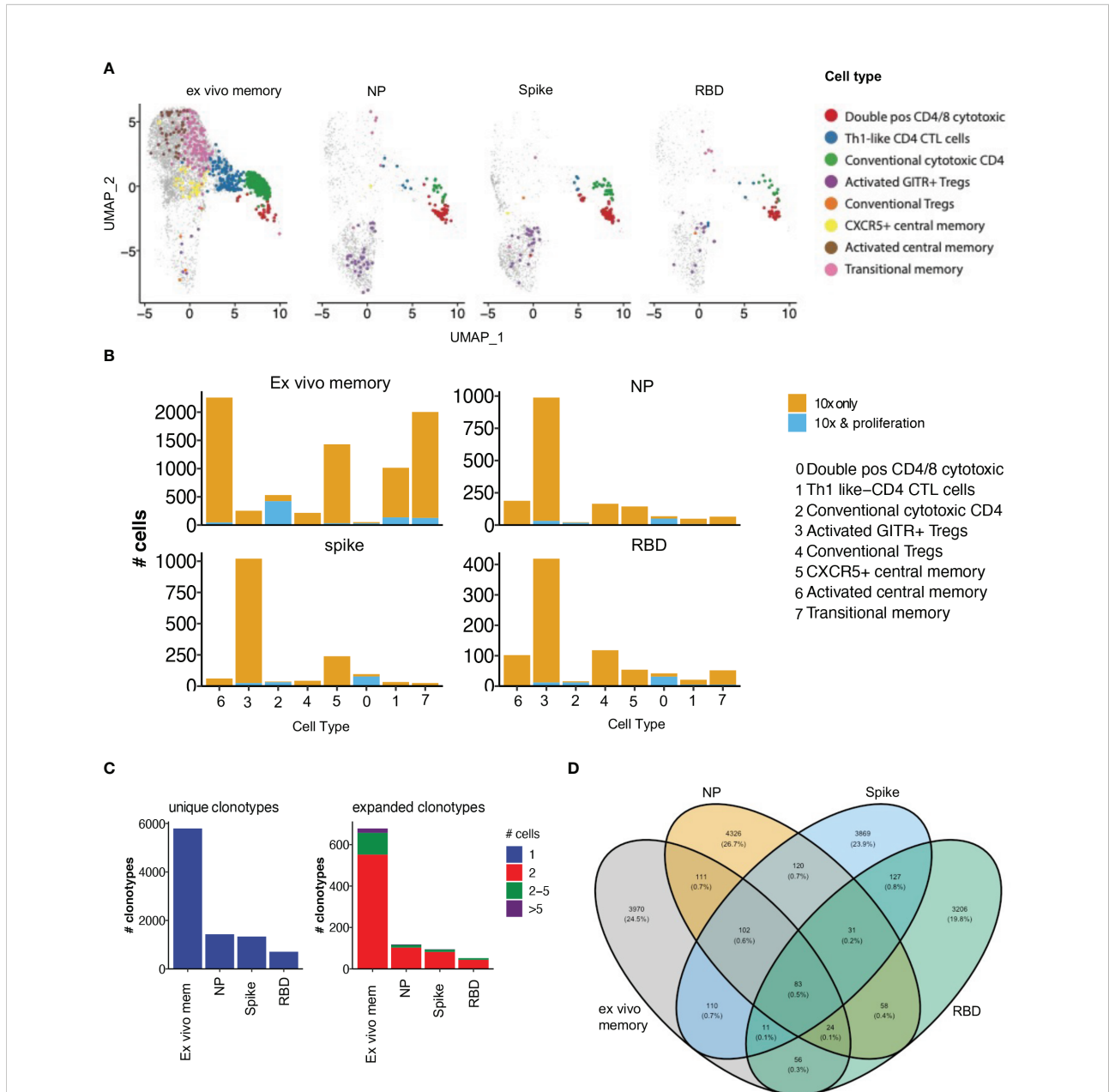


FIGURE 7

Proliferative clonotypes are enriched within Tregs and cytotoxic subsets. Bulk TCR sequencing of CD4s T cells from Ab high subjects that proliferated for 5 days following stimulation with SARS-CoV-2 peptide pools were matched with 10x single-cell TCRs to examine enriched clonotypes. (A) UMAP clonotypes that were enriched following proliferation and matched to 10x TCRs and split into 4 conditions: ex vivo memory, nucleoprotein (NP), Spike and RBD. (B) Proliferative CD4 clones were highly enriched with activated GTR+ Tregs and cytotoxic clusters. (C) Abundance of unique single clonotypes with few expanded clonotypes within stimulated conditions. (D) Minimal shared TCR clonotypes within stimulated conditions compared to ex vivo memory. Fishers exact test with Bonferroni's corrected *p* values shown for log odd ratios.

Figure 7B), (ii) CD4/CD8 double positive CTL (cluster 0; Figure 7B); and (iii) relatively limited proliferation of activated GTR+ Tregs, compared to their identification in the OX40 assay 10x only analysis (cluster 3; Figure 7B). The majority of clonotypes identified through the single cell RNAseq analysis were unique singletons, while expanded clonotypes following proliferation consisted mostly of 2 cells with the same clonotype, as well as a small portion of clonotypes that were 2-5 cells (Figure 7C).

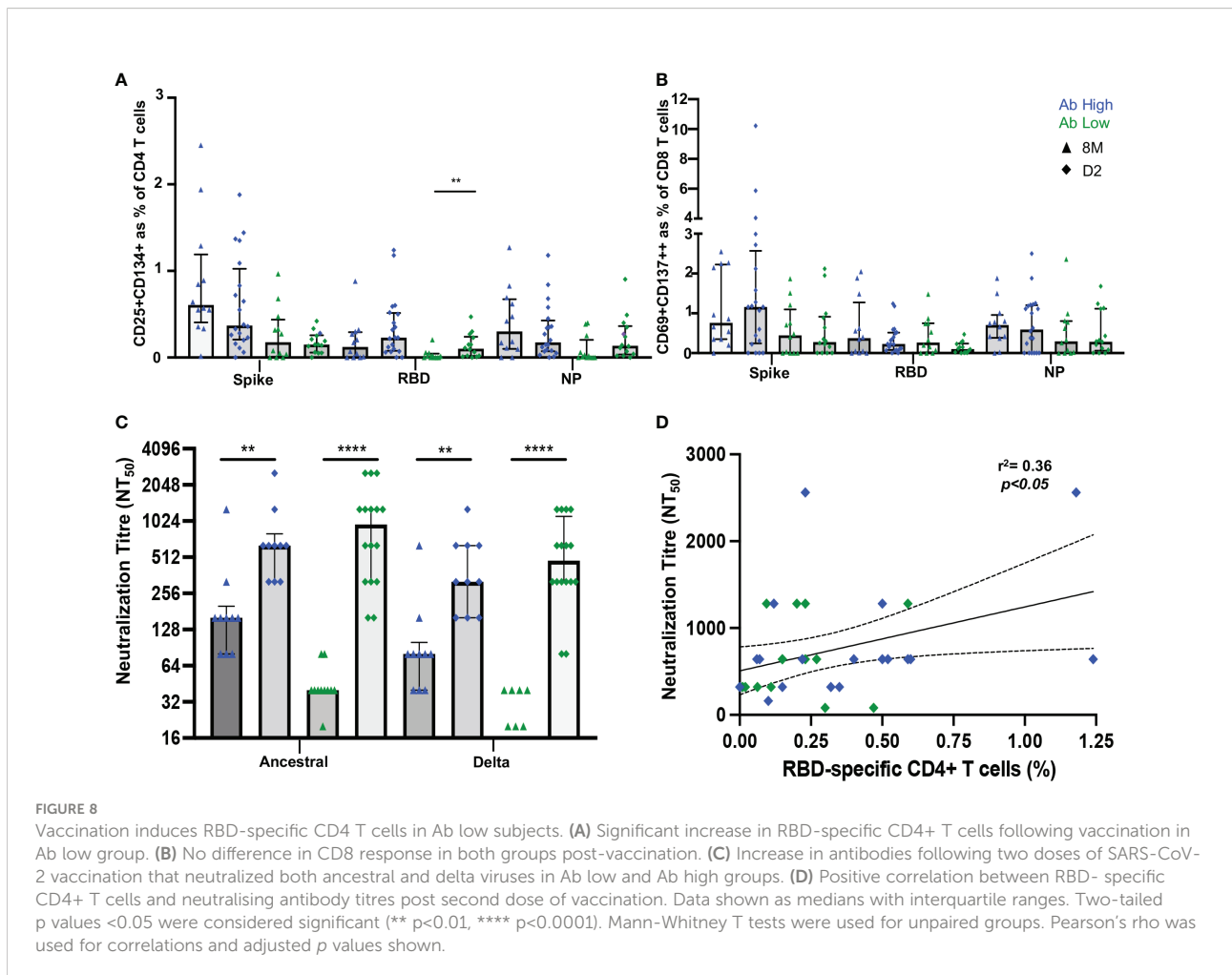
As expected, there was very little overlap of TCR clonotypes between the different antigen-specific responses, with <1% of clonotypes being shared (Figure 7D), consistent with high diversity within SARS-CoV-2 reactive CD4 T cells. A total of 3,599 unique SARS-CoV-2 clonotypes were identified in our study that have not been previously reported elsewhere.

### 3.7 Increased RBD-specific CD4 T cells following vaccination

It was then important to assess whether vaccination would improve adaptive immune responses in the low antibody

ADAPT convalescent subjects. Between 2 and 4 weeks following the vaccination second dose of either BNT162b2 or ChAdOx1, PBMC samples were collected from the previously infected participants, from either the high or low antibody patient groups, respectively. No longitudinal difference was observed between either spike or NP-specific CD4 T cell responses at D2 timepoint (2-4 weeks post-second dose) in both subject groups. However, in RBD-specific responses, in the original Ab low group, there was a 3.4-fold increase from the 8-month convalescent timepoint to the post-vaccination D2 timepoint ( $p < 0.01$ ; Figure 8A). No difference was observed in CD8 T cell response between pre or post vaccination timepoints (Figure 8B).

A sharp increase in neutralizing antibody titres towards the ancestral strain was observed in both Ab high and low groups after vaccination (Ab high 8M  $NT_{50} = 160$ , D2  $NT_{50} = 640$  [ $p < 0.01$ ]; Ab low 8M  $NT_{50} = 40$ , D2  $NT_{50} = 960$  [ $p < 0.0001$ ]). Neutralization of the B.1.617.2 delta strain was also increased (Ab high 8M  $NT_{50} = 80$ , D2  $NT_{50} = 320$  [ $p < 0.01$ ]; Ab low 8M  $NT_{50} = 0$ , D2  $NT_{50} = 480$  [ $p < 0.0001$ ]) (Figure 8C). As it was previously shown that low RBD-specific





CD4 T cells response was associated with low neutralizing antibodies at 3- and 8-months post-infection, it was important to correlate these two parameters at the post-vaccination timepoint. A positive correlation (spearman's  $\rho=0.36$ ,  $p<0.05$ ) was observed between RBD-specific CD4 T cells in the OX40 assay and neutralization titre at the D2 post-second dose timepoint (Figure 8D).

## 4 Discussion

This study has revealed that those only those convalescent COVID-19 patients who had readily detectable RBD-specific CD4 T cell *in vitro* recall responses had significantly higher neutralizing antibody titres, whereas lower anti-spike antibody levels, especially neutralizing antibody titres, were associated with a lack of RBD-specific proliferative CD4 T cells. These results raise serious questions of the quality and quantity of any immediate anamnestic *in vivo* response in patients without these proliferative CD4 T cell responses, if re-exposed to SARS-CoV-2. In contrast, those patients with *in vitro* proliferative RBD-specific CD4 T cells would be predicted to mount an early vigorous *in vivo* immune response if re-exposed. Other groups using similar assays to our OX40 assay (7, 14–18) have also found that the majority of recovered COVID-19 patients had detectable responses to pools of spike peptides, but with only a subset of patients having CD4 T cell responses to RBD epitopes. We have also previously shown that early CD4+ T cell responses can predict RBD-specific memory B cell frequencies at 1-year post-infection (57).

It is widely believed that neutralizing antibodies are the first line of defence against re-infection with the same viral pathogen (4). Our results agree with other studies that there is a very large variation in levels of such neutralizing antibodies in the serum of individuals recovered from COVID-19 and their longevity (6, 7, 35); the reasons for this range of responses were unclear, but the quantity and quality of viral antigen-specific CD4 T cells are highly likely to be important (5). Furthermore, it is unknown what level of such antibodies are required for complete protection. However, with the current vaccines, and evidence from their Phase III trials, a correlation of higher neutralization titres and lower infection rates has been reported (58).

Our results directly correlated RBD-specific proliferative CD4 T cell responses in convalescent PBMC with anti-spike antibodies and neutralizing antibody titres. Furthermore, in the recovered COVID-19 subjects with low antibody levels, their spike-specific CD4 T cells showed very little proliferative response *in vitro*, and in the small number of cells that did proliferate, they appeared to relatively highly express the Treg transcription factor Foxp3. Our CD25/OX40 assay was able to identify SARS-CoV-2-specific Tregs, using CD39 expression (56), which was confirmed at the transcriptional level with Foxp3 and GITR expression. Treg responses have been under-

represented in other studies using other activation markers, namely CD40L (CD154) and 4-1BB (CD137) (24, 59–61), together with shorter incubations with antigens, that did not pick up these important regulatory cells. Further studies are needed to understand whether a preponderance of Tregs exerts a greater influence over a smaller number of spike-specific proliferation-capable CD4 T cells from the Ab low subjects.

When SARS-CoV-2 spike-, RBD- and NP-specific CD4 T cells from patients from the high Ab group were examined at the single cell transcriptomic level, heterogeneous profiles of CD4 T cell subsets were observed that included central memory cells and CD4 CTL, as well as regulatory T cell populations expressing GITR and Foxp3. Importantly, this contrasts with the specific CD4 and CD8 T cells from patients from the antibody low group which showed a predominance of expression of Foxp3 and CTLA-4, respectively, associated with their limited proliferative responses. We have previously reported high CTLA-4 expression in HIV-specific CD4 T cells (62) which was inhibitory to proliferative responses *in vitro* (63), whereas vaccinia-specific CD4 T cells expressed less CTLA-4 and proliferated well, 21 days after inoculation (9). Interestingly, one study has reported an immunodominant CD4 epitope within RBD, using proliferation *in vitro* in response to spike peptides, in convalescent PBMC, as an initial step in a cloning procedure (21), but antibody levels were not reported.

T follicular helper cells (Tfh) are vital in B cell maturation and immunoglobulin class switching within the germinal centre (5). Two studies have suggested that circulating Tfh (cTfh) from recovered COVID-19 patients include spike-specific CD4 T, but in one study RBD-specific cTfh were rare (14) while in the other, total spike-specific cTfh were only seen in 3/26 subjects (64), overall consistent with a large proportion of immunodominant epitopes for the spike-specific CD4 T cells being outside the RBD (14, 65).

We were able to characterize in detail the expanded RBD-specific CD4 T cells after *in vitro* proliferation and, surprisingly, we found no staining for the Tfh-defining transcription factor Bcl6 in the expanded cells from PBMC, despite using staining protocols that readily identified Bcl6+ Tfh and germinal centre B cells in other studies of lymph node (66, 67) and tonsil cells (68). In a previous study, we had identified *BCL6* at the single cell level in antigen-specific CD4 T cells in PBMC (69). Therefore, we postulated that spike-specific cTfh cells should be encompassed within the CXCR5+ and activated central memory subsets, observed from our single cell RNAseq data, but low transcript expression of *BCL6* did not give us a definitive answer. Nevertheless, future *in vitro* studies should examine whether memory CD4 T cells in PBMC, in particular cTfh, from recovered COVID-19 patients, can boost anti-spike antibodies by memory B cells *in vitro*, analogous to previous studies for other recall antigens (70).

Instead, our analysis of proliferated RBD-specific CD4 T cells showed they were more likely to highly express T-bet, the Th1-defining transcription factor. Most studies have reported that IFN- $\gamma$

is the most prominent cytokine produced by SARS-CoV-2 specific memory T cells *in vitro* in response to antigen (14–17), so expression of T-bet in expanded cells is consistent with a Th1 skewing of spike-specific effector CD4 T cells in PBMC.

We have previously shown that there are relatively high expression of cytotoxic lymphocyte markers in HIV-specific and CMV-specific CD4 T cells (71–73), as well as CD4 CTL found in other viral infections (reviewed recently in (74)). Very early following vaccinia inoculation, many vaccinia-specific CD4 T cells were also CTL, expressing mainly Granzyme K, at day 14, at the same time as the peak of activated CD4 T cells in blood (10), consistent with what was reported for a COVID-19 patient during the acute phase of the infection (75). We identified three transcriptomic clusters of cytotoxic CD4 T cells that were within the SARS-CoV-2 reactive subsets by single cell RNAseq. This observation was consistent with our finding of *in vitro* expanded spike-specific CD4 T cells that expressed protein markers of cytotoxic T lymphocytes (CTL), including the granzymes A and B, and perforin, and cytotoxic granules (as defined by the antibody TIA-1, which recognizes the protein encoded by the gene *NKG7* (71, 76)). Highly enriched proliferative clonotypes were also shown to overlap with conventional CD4 CTL and CD4/8 double positive CD4 CTL by single cell RNAseq. It was also evident following bulk TCR-seq that proliferated clonotypes in response to spike and RBD were enriched within CD4 CTL clusters. Effector CD4 T cells expressing cytotoxic granules have been identified in other single cell transcriptomic studies (61, 77), suggesting that CD4 CTLs may play an important role in eliminating SARS-CoV-2 infected cells.

Based on what is known about CD4 T cell help for B cell responses (5), it is highly likely that memory CD4 T cells in peripheral blood reflect a large CD4 T cell response in draining lymph nodes, which includes T follicular helper cells (Tfh), but also results in exit of antigen-specific effector and memory cells into the circulation. We have directly observed these highly activated, non-Tfh cells in lymph nodes in untreated HIV-1 infection (66, 68), but their clonal relationship to similarly elevated Tfh cells is still under study.

From the current study, it isn't clear at the molecular level why CD4 T cells with specificities to epitopes within RBD may generate better levels of anti-spike neutralizing antibodies. Theoretically, any spike-specific CD4 T cells should be able to help B cells that are able to take up spike protein *via* specificity for RBD. However, spike protein is very large and is designed to be cleaved during viral entry into target cells, involving multiple proteases (78–80), so it is possible that spike available for B cell recognition in germinal centres may also be cleaved to smaller protein fragments, only some of which link B cell and T cell epitopes around RBD.

Clearly this needs further study with defined epitopes, along with the clonal relationships between germinal centre Tfh cells during acute infection and memory cells during convalescence. Early studies in murine models of influenza infection suggested

that there might be “intermolecular” CD4 help for antibody responses, where the CD4 T cells and B cells recognized different protein antigens (81, 82). However, in a vaccinia virus mouse model it was shown clearly that “intramolecular” CD4 help was required for antibodies to each individual viral protein from this large poxvirus (83). Most studies of SARS-CoV-2 specific T cells have used large peptide pools, whereas we have found most of our associations with recombinant proteins, which may be an advantage because it requires the full antigen-processing and HLA Class II presentation pathway rather than extracellular saturation with a large number of exogenous peptides. Finally, it also has to be considered whether some RBD epitopes may be obscured by glycan residues that lock the RBD in a “down” position (84), since our recombinant proteins were made in human cell lines (31) and thereby correctly glycosylated.

Possible reasons why some infected individuals have low overall adaptive immune responses could be due to (i) lower initial viral loads during first wave infections compared to later waves of variants (85); and (ii) possibly having more inhibitory and/or exhausted B and T cells (24); but lower RBD-specific responses could result if antigen presentation to CD4 T cells is dominated by epitopes in spike fragments outside of RBD (65, 86).

Importantly, however, it appears that RBD-specific CD4 T cells could be boosted to some extent by vaccination. A very recently published study of vaccination shows an association between carriage of the HLA-DQB1\*06 allele and combined higher antibody and CD4 T cell proliferation responses to RBD, following vaccination, which was postulated to be due to improved presentation of an epitope adjacent to the RBD (87). Our results suggest that booster efficacy would be improved by concentrating on CD4 T cell epitopes in and around the RBD, which may be the optimal regimen for generation and longevity of neutralizing antibodies.

## Data availability statement

The datasets presented in this study can be found in online repositories. The names of the repository/repositories and accession number(s) can be found below: <http://www.ncbi.nlm.nih.gov/bioproject/877691>.

## Ethics statement

The ADAPT study was approved by the St. Vincent's Hospital Human Research Ethics Committee (2020/ETH00964) and is a registered trial (ACTRN12620000554965). ADAPT-C sub study was approved by the same committee (2020/ETH01429). All data were stored using REDCap electronic data capture tools. Unexposed healthy adult donors

were recruited through St. Vincent's Hospital which was approved by St Vincent's Hospital Human Research Ethics Committee (HREC/13/SVH/145 and HREC/10/SVH/130). All participants gave written informed consent. The patients/participants provided their written informed consent to participate in this study.

## Author contributions

Protocol design and clinical management: GM, GD, DD. Experimental design and procedures: CP, WK, KJ, VK, AH, AA, AAg, VM, AS, RR, PS, MLF, HL, TD, MS, CM, FB-T, ST, TP, AK, JZ. Visualization: CP, WK, KJ, JZ. Funding acquisition: GM, GD, DD, DC, ST, FB-T, TP, PC, AK, JZ. Supervision: DC, ST, PC, GM, PC, TP, AK. Writing – original draft: CP, WK, KJ, TP, JZ. Writing – review & editing: CP, WK, KJ, CM, ST, AA, TP, AK, JZ. All authors contributed to the article and approved the submitted version.

## Funding

St Vincent's Clinic Foundation Grant (GM, GD, DD) Medical Research Future Fund Grant (ST, FB-T, TP, JZ) National Health and Medical Research Council (NHMRC) Program Grant ID1149990 (AK) NHMRC Fellowship ID1155678 (TP) UNSW Cellular Genomics Futures Institute Seed Funding (WK) Mrs. Janice Gibson and the Ernest Heine Family Foundation (PC and TP) Garvan Institute COVID Catalytic Grant (TP) UNSW COVID-19 Rapid Response Research Initiative (TP)

## References

- Hansen CH, Michlmayr D, Gubbels SM, Mølbak K, Ethelberg S. Assessment of protection against reinfection with SARS-CoV-2 among 4 million PCR-tested individuals in Denmark in 2020: a population-level observational study. *Lancet* (2021) 397:1204–12. doi: 10.1016/S0140-6736(21)00575-4
- Altarawneh HN, Chemaitelly H, Hasan MR, Ayoub HH, Qassim S, AlMukdad S, et al. Protection against the omicron variant from previous SARS-CoV-2 infection. *New Engl J Med* (2022) 386:1288–90. doi: 10.1056/NEJMc2200133
- Fontanet A, Cauchemez S. COVID-19 herd immunity: Where are we? *Nat Rev Immunol* (2020) 20: 583–584. doi: 10.1038/s41577-020-00451-5
- Nabel GJ. Designing tomorrow's vaccines. *N Engl J Med* (2013) 368:551–60. doi: 10.1056/NEJMr1204186
- Crotty S. Follicular helper CD4 T cells (TFH). *Annu Rev Immunol* (2011) 29:621–63. doi: 10.1146/annurev-immunol-031210-101400
- Xiang T, Liang B, Fang Y, Lu S, Li S, Wang H, et al. Declining levels of neutralizing antibodies against SARS-CoV-2 in convalescent COVID-19 patients one year post symptom onset. *Front Immunol* (2021) 12:708523. doi: 10.3389/fimmu.2021.708523
- Dan JM, Mateus J, Kato Y, Hastie KM, Yu ED, Faliti CE, et al. Immunological memory to SARS-CoV-2 assessed for up to eight months after infection. *bioRxiv* (2020) 371: (6529). doi: 10.1101/2020.11.15.383323
- Painter MM, Mathew D, Goel RR, Apostolidis SA, Pattekar A, Kuthuru O, et al. Rapid induction of antigen-specific CD4(+) T cells is associated with

## Acknowledgments

The authors thank Bertha Fsadni, Sri Meka, Julie Jurczyk and Kate Merlin at the St. Vincent's Institute for Applied Medical Research-Clinical Trials Unit for their expertise in specimen processing and bio-banking. We thank Dr. Emma Johansson Beves for assistance on the Cytek Aurora.

## Conflict of interest

The authors declare that the research was conducted in the absence of any commercial or financial relationships that could be construed as a potential conflict of interest.

## Publisher's note

All claims expressed in this article are solely those of the authors and do not necessarily represent those of their affiliated organizations, or those of the publisher, the editors and the reviewers. Any product that may be evaluated in this article, or claim that may be made by its manufacturer, is not guaranteed or endorsed by the publisher.

## Supplementary material

The Supplementary Material for this article can be found online at: <https://www.frontiersin.org/articles/10.3389/fimmu.2022.1032911/full#supplementary-material>

coordinated humoral and cellular immunity to SARS-CoV-2 mRNA vaccination. *Immunity* (2021) 54:2133–2142 e2133. doi: 10.1016/j.immuni.2021.08.001

9. Zaunders JJ, Dyer WB, Munier ML, Ip S, Liu J, Amyes E, et al. CD127+ CCR5+CD38+++ CD4+ Th1 effector cells are an early component of the primary immune response to vaccinia virus and precede development of interleukin-2+ memory CD4+ T cells. *J Virol* (2006) 80:10151–61. doi: 10.1128/JVI.02670-05

10. Munier CM, van Bockel D, Bailey M, Ip S, Xu Y, Alcantara S, et al. The primary immune response to vaccinia virus vaccination includes cells with a distinct cytotoxic effector CD4 T-cell phenotype. *Vaccine* (2016) 34:5251–61. doi: 10.1016/j.vaccine.2016.09.009

11. Hammarlund E, Lewis MW, Hansen SG, Strelow LI, Nelson JA, Sexton GJ, et al. Duration of antiviral immunity after smallpox vaccination. *Nat Med* (2003) 9:1131–7. doi: 10.1038/nm917

12. Doherty PC, Christensen JP. Accessing complexity: the dynamics of virus-specific T cell responses. *Annu Rev Immunol* (2000) 18:561–92. doi: 10.1146/annurev.immunol.18.1.561

13. Zaunders J, van Bockel D. Innate and adaptive immunity in long-term non-progression in HIV disease. *Front Immunol* (2013) 4:95. doi: 10.3389/fimmu.2013.00095

14. Juno JA, Tan HX, Lee WS, Reynaldi A, Kelly HG, Wragg K, et al. Humoral and circulating follicular helper T cell responses in recovered patients with COVID-19. *Nat Med* (2020) 26:1428–34. doi: 10.1038/s41591-020-0995-0

15. Grifoni A, Weiskopf D, Ramirez SI, Mateus J, Dan JM, Moderbacher CR, et al. Targets of T cell responses to SARS-CoV-2 coronavirus in humans with COVID-19 disease and unexposed individuals. *Cell* (2020) 181:1489–1501 e1415. doi: 10.1016/j.cell.2020.05.015
16. Ni L, Ye F, Cheng ML, Feng Y, Deng YQ, Zhao H, et al. Detection of SARS-CoV-2-specific humoral and cellular immunity in COVID-19 convalescent individuals. *Immunity* (2020) 52:971–977 e973. doi: 10.1016/j.immuni.2020.04.023
17. Weiskopf D, Schmitz KS, Raadsen MP, Grifoni A, Okba NMA, Endeman H, et al. Phenotype and kinetics of SARS-CoV-2-specific T cells in COVID-19 patients with acute respiratory distress syndrome. *Sci Immunol* (2020) 5(48). doi: 10.1126/sciimmunol.abd2071
18. Braun J, Loyal L, Frensch M, Wendisch D, Georg P, Kurth F, et al. SARS-CoV-2-reactive T cells in healthy donors and patients with COVID-19. *Nature* (2020) 587:270–274. doi: 10.1038/s41586-020-2598-9
19. Jung JH, Rha MS, Sa M, Choi HK, Jeon JH, Seok H, et al. SARS-CoV-2-specific T cell memory is sustained in COVID-19 convalescent patients for 10 months with successful development of stem cell-like memory T cells. *Nat Commun* (2021) 12:4043. doi: 10.1038/s41467-021-24377-1
20. Zaunders JJ, Munier ML, Seddiki N, Pett S, Ip S, Bailey M, et al. High levels of human antigen-specific CD4+ T cells in peripheral blood revealed by stimulated coexpression of CD25 and CD134 (OX40). *J Immunol* (2009) 183:2827–36. doi: 10.4049/jimmunol.0803548
21. Low JS, Vaquerinho D, Mele F, Foglierini M, Jerak J, Perotti M, et al. Clonal analysis of immunodominance and cross-reactivity of the CD4 T cell response to SARS-CoV-2. *Science* (2021) 372:1336–41. doi: 10.1126/science.abg8985
22. Schmidt ME, Varga SM. The CD8 T cell response to respiratory virus infections. *Front Immunol* (2018) 9:678. doi: 10.3389/fimmu.2018.00678
23. Rha MS, Shin EC. Activation or exhaustion of CD8(+) T cells in patients with COVID-19. *Cell Mol Immunol* (2021) 18:2325–33. doi: 10.1038/s41423-021-00750-4
24. Kusnadi A, Ramirez-Suastegui C, Fajardo V, Chee SJ, Meckiff BJ, Simon H, et al. Severely ill COVID-19 patients display impaired exhaustion features in SARS-CoV-2-reactive CD8(+) T cells. *Sci Immunol* (2021) 6(55). doi: 10.1126/sciimmunol.abe4782
25. Gimenez E, Albert E, Torres I, Remigia MJ, Alcaraz MJ, Galindo MJ, et al. SARS-CoV-2-reactive interferon-gamma-producing CD8+ T cells in patients hospitalized with coronavirus disease 2019. *J Med Virol* (2021) 93:375–82. doi: 10.1002/jmv.26213
26. Lineburg KE, Grant EJ, Swaminathan S, Chatzileontiadou DSM, Szeto C, Sloane H, et al. CD8(+) T cells specific for an immunodominant SARS-CoV-2 nucleocapsid epitope cross-react with selective seasonal coronaviruses. *Immunity* (2021) 54:1055–1065 e1055. doi: 10.1016/j.immuni.2021.04.006
27. Schulten I, Kemming J, Oberhardt V, Wild K, Seidel LM, Killmer S, et al. Characterization of pre-existing and induced SARS-CoV-2-specific CD8(+) T cells. *Nat Med* (2021) 27:78–85. doi: 10.1038/s41591-020-01143-2
28. Nguyen THO, Rowntree LC, Petersen J, Chua BY, Hensen L, Kedzierski L, et al. CD8(+) T cells specific for an immunodominant SARS-CoV-2 nucleocapsid epitope display high naive precursor frequency and TCR promiscuity. *Immunity* (2021) 54:1066–1082 e1065. doi: 10.1016/j.immuni.2021.04.009
29. Darley DR, Dore GJ, Cysique L, Wilhelm KA, Andresen D, Tonga K, et al. Persistent symptoms up to four months after community and hospital-managed SARS-CoV-2 infection. *Med J Aust* (2021) 214:279–80. doi: 10.5694/mja2.50963
30. Phetsouphanh C, Darley DR, Wilson DB, Howe A, Munier CML, Patel SK, et al. Immunological dysfunction persists for 8 months following initial mild-to-moderate SARS-CoV-2 infection. *Nat Immunol* (2022) 23:210–6. doi: 10.1038/s41590-021-01113-x
31. Rouet R, Mazigi O, Walker GJ, Langley DB, Sobti M, Schofield P, et al. Potent SARS-CoV-2 binding and neutralization through maturation of iconic SARS-CoV-1 antibodies. *MAbs* (2021) 13:1922134. doi: 10.1080/19420862.2021.1922134
32. Zaunders J, Munier CML, McGuire HM, Law H, Howe A, Xu Y, et al. Mapping the extent of heterogeneity of human CCR5+ CD4+ T cells in peripheral blood and lymph nodes. *AIDS* (2020) 34:833–48. doi: 10.1097/QAD.0000000000002503
33. Hsu DC, Zaunders JJ, Plit M, Leeman C, Ip S, Iampornsin T, et al. A novel assay detecting recall response to mycobacterium tuberculosis: Comparison with existing assays. *Tuberculosis (Edinb)* (2012) 92:321–7. doi: 10.1016/j.tube.2012.03.008
34. Zaunders J, Dyer W, Churchill M, Munier C, Cunningham P, Suzuki K, et al. Possible clearance of transfusion-acquired nef/LTR-deleted attenuated HIV-1 infection by an elite controller with CCR5 Δ32 heterozygous and HLA-B57 genotype. *J Virus Eradication* (2019) 5:73–83. doi: 10.1016/S2055-6640(20)30056-X
35. Tea F, Ospina Stella A, Aggarwal A, Ross Darley D, Pilli D, Vitale D, et al. SARS-CoV-2 neutralizing antibodies: Longevity, breadth, and evasion by emerging viral variants. *PLoS Med* (2021) 18:e1003656. doi: 10.1371/journal.pmed.1003656
36. Follenzi A, Naldini L. *Gene therapy protocols*. Morgan JR, editor. Totowa, NJ: Springer New York (2002) p. 259–74.
37. Aggarwal A, Stella A, Walker G, Akerman A, Esneau C, Milogiannakis V, et al. Platform for isolation and characterization of SARS-CoV-2 variants enables rapid characterisation of omicron in Australia. *Nat Microbiol* (2022) 7(6):896–908. doi: 10.1038/s41564-022-01135-7
38. Stoeckius M, Hafemeister C, Stephenson W, Houck-Loomis B, Chattopadhyay PK, Swerdlow H, et al. Simultaneous epitope and transcriptome measurement in single cells. *Nat Methods* (2017) 14:865–8. doi: 10.1038/nmeth.4380
39. Stuart T, Butler A, Hoffman P, Hafemeister C, Papalexi E, Mauck WM3rd, et al. Comprehensive integration of single-cell data. *Cell* (2019) 177:1888–1902 e1821. doi: 10.1016/j.cell.2019.05.031
40. Hafemeister C, Satija R. Normalization and variance stabilization of single-cell RNA-seq data using regularized negative binomial regression. *Genome Biol* (2019) 20:296. doi: 10.1186/s13059-019-1874-1
41. Lun AT, McCarthy DJ, Marioni JC. A step-by-step workflow for low-level analysis of single-cell RNA-seq data with bioconductor. *F1000Res* (2016) 5:2122. doi: 10.12688/f1000research.9501.2
42. McCarthy DJ, Campbell KR, Lun AT, Wills QF. Scater: pre-processing, quality control, normalization and visualization of single-cell RNA-seq data in R. *Bioinformatics* (2017) 33:1179–86. doi: 10.1093/bioinformatics/btw777
43. Law CW, Chen Y, Shi W, Smyth GK. Voom: Precision weights unlock linear model analysis tools for RNA-seq read counts. *Genome Biol* (2014) 15:R29. doi: 10.1186/gb-2014-15-2-r29
44. Massey J, Jackson K, Singh M, Hughes B, Withers B, Ford C, et al. Haematopoietic stem cell transplantation results in extensive remodelling of the clonal T cell repertoire in multiple sclerosis. *Front Immunol* (2022) 13. doi: 10.3389/fimmu.2022.798300
45. Vander Heiden JA, Yaari G, Uduman M, Stern JNH, O'Connor KC, Hafler DA, et al. pRESTO: a toolkit for processing high-throughput sequencing raw reads of lymphocyte receptor repertoires. *Bioinformatics* (2014) 30:1930–2. doi: 10.1093/bioinformatics/btu138
46. Ye J, Ma N, Madden TL, Ostell JM. IgBLAST: an immunoglobulin variable domain sequence analysis tool. *Nucleic Acids Res* (2013) 41:W34–40. doi: 10.1093/nar/gkt382
47. Gupta NT, Vander Heiden JA, Uduman M, Gadala-Maria D, Yaari G, Kleinstein SH. Change-O: a toolkit for analyzing large-scale B cell immunoglobulin repertoire sequencing data. *Bioinformatics* (2015) 31:3356–8. doi: 10.1093/bioinformatics/btv359
48. Hao Y, Hao S, Andersen-Nissen E, Mauck WM3rd, Zheng S, Butler A, et al. Integrated analysis of multimodal single-cell data. *Cell* (2021) 184:3573–3587.e3529. doi: 10.1016/j.cell.2021.04.048
49. Wickham H, Averick M, Bryan J, Chang W, McGowan L, François R, et al. Welcome to the tidyverse. *J Open Source Software* (2019) 4. doi: 10.21105/joss.01686
50. Shannon CE. A mathematical theory of communication. *Bell System Tech J* (1948) 27:379–423. doi: 10.1002/j.1538-7305.1948.tb01338.x
51. Marcon E, Héroult B. Entropart: An R package to measure and partition diversity. *J Stat Software* (2015) 67:1–26. doi: 10.18637/jss.v067.i08
52. Krzywinski M, Schein J, Birol I, Connors J, Gascogne R, Horsman D, et al. Circos: an information aesthetic for comparative genomics. *Genome Res* (2009) 19:1639–45. doi: 10.1101/gr.092759.109
53. Nolan S, Vignali M, Klinger M, Dines JN, Kaplan IM, Svejnoha E, et al. A large-scale database of T-cell receptor beta (TCRβ) sequences and binding associations from natural and synthetic exposure to SARS-CoV-2. *Res Sq* (2020). doi: 10.21203/rs.3.rs-51964/v1
54. Bagaev DV, Vroomans RMA, Samir J, Stervbo U, Rius C, Dolton G, et al. VDJdb in 2019: Database extension, new analysis infrastructure and a T-cell receptor motif compendium. *Nucleic Acids Res* (2019) 48:D1057–62. doi: 10.1093/nar/gkz874
55. Wolf M, Kuball J, Ho WY, Nguyen H, Manley TJ, Bleakley M, et al. Activation-induced expression of CD137 permits detection, isolation, and expansion of the full repertoire of CD8+ T cells responding to antigen without requiring knowledge of epitope specificities. *Blood* (2007) 110:201–10. doi: 10.1182/blood-2006-11-056168
56. Seddiki N, Cook L, Hsu DC, Phetsouphanh C, Brown K, Xu Y, et al. Human antigen-specific CD4(+) CD25(+) CD134(+) CD39(+) T cells are enriched for regulatory T cells and comprise a substantial proportion of recall responses. *Eur J Immunol* (2014) 44:1644–61. doi: 10.1002/eji.201344102

57. Balachandran H, Phetsouphanh C, Agapiou D, Adhikari A, Rodrigo C, Hammoud M, et al. Maintenance of broad neutralizing antibodies and memory b cells 1 year post-infection is predicted by SARS-CoV-2-specific CD4+ T cell responses. *Cell Rep* (2022) 38:110345. doi: 10.1016/j.celrep.2022.110345
58. Khoury DS, Cromer D, Reynaldi A, Schlub TE, Wheatley AK, Juno JA, et al. Neutralizing antibody levels are highly predictive of immune protection from symptomatic SARS-CoV-2 infection. *Nat Med* (2021) 27:1205–11. doi: 10.1038/s41591-021-01377-8
59. Dan JM, Mateus J, Kato Y, Hastie KM, Yu ED, Faliti CE, et al. Immunological memory to SARS-CoV-2 assessed for up to 8 months after infection. *Science* (2021) 371. doi: 10.1126/science.abc4063
60. Mateus J, Grifoni A, Tarke A, Sidney J, Ramirez SI, Dan JM, et al. Selective and cross-reactive SARS-CoV-2 T cell epitopes in unexposed humans. *Science* (2020) 370(6512):89–94. doi: 10.1126/science.abd3871
61. Meckiff BJ, Ramirez-Suastegui C, Fajardo V, Chee SJ, Kusnadi A, Simon H, et al. Single-cell transcriptomic analysis of SARS-CoV-2 reactive CD4 (+) T cells. *SSRN* (2020), 3641939. doi: 10.1101/2020.06.12.148916
62. Zaunders JJ, Ip S, Munier ML, Kaufmann DE, Suzuki K, Brereton C, et al. Infection of CD127+ (interleukin-7 receptor+) CD4+ cells and overexpression of CTLA-4 are linked to loss of antigen-specific CD4 T cells during primary human immunodeficiency virus type 1 infection. *J Virol* (2006) 80:10162–72. doi: 10.1128/JVI.00249-06
63. Kaufmann DE, Kavanagh DG, Pereyra F, Zaunders JJ, Mackey EW, Miura T, et al. Upregulation of CTLA-4 by HIV-specific CD4(+) T cells correlates with disease progression and defines a reversible immune dysfunction. *Nat Immunol* (2007) 8:1246–54. doi: 10.1038/ni1515
64. Boppana S, Qin K, Files JK, Russell RM, Stoltz R, Bibollet-Ruche F, et al. SARS-CoV-2-specific circulating T follicular helper cells correlate with neutralizing antibodies and increase during early convalescence. *PLoS Pathog* (2021) 17: e1009761. doi: 10.1371/journal.ppat.1009761
65. Tarke A, Sidney J, Kidd CK, Dan JM, Ramirez SI, Yu ED, et al. Comprehensive analysis of T cell immunodominance and immunoprevalence of SARS-CoV-2 epitopes in COVID-19 cases. *Cell Rep Med* (2021) 2:100204. doi: 10.1016/j.xcrm.2021.100204
66. Hey-Nguyen WJ, Xu Y, Pearson CF, Bailey M, Suzuki K, Tantau R, et al. Quantification of residual germinal center activity and HIV-1 DNA and RNA levels using fine needle biopsies of lymph nodes during antiretroviral therapy. *AIDS Res Hum Retroviruses* (2017) 33:648–57. doi: 10.1089/aid.2016.0171
67. Law H, Mach M, Howe A, Obeid S, Milner B, Carey C, et al. Early expansion of CD38+ICOS+ GC tfh in draining lymph nodes during influenza vaccination immune response. *iScience* (2022) 25:103656. doi: 10.1016/j.isci.2021.103656
68. Xu Y, Phetsouphanh C, Suzuki K, Aggarwal A, Graff-Dubois S, Roche M, et al. HIV-1 and SIV predominantly use CCR5 expressed on a precursor population to establish infection in T follicular helper cells. *Front Immunol* (2017) 8:376. doi: 10.3389/fimmu.2017.00376
69. Phetsouphanh C, Xu Y, Amin J, Seddiki N, Procopio F, Sekaly RP, et al. Characterization of transcription factor phenotypes within antigen-specific CD4+ T cells using qualitative multiplex single-cell RT-PCR. *PLoS One* (2013) 8:e74946. doi: 10.1371/journal.pone.0074946
70. Morita R, Schmitt N, Bentebibel SE, Ranganathan R, Bourdery L, Zurawski G, et al. Human blood CXCR5(+)-CD4(+) T cells are counterparts of T follicular cells and contain specific subsets that differentially support antibody secretion. *Immunity* (2011) 34:108–21. doi: 10.1016/j.immuni.2010.12.012
71. Zaunders JJ, Dyer WB, Wang B, Munier ML, Miranda-Saksena M, Newton R, et al. Identification of circulating antigen-specific CD4+ T lymphocytes with a CCR5+, cytotoxic phenotype in an HIV-1 long-term nonprogressor and in CMV infection. *Blood* (2004) 103:2238–47. doi: 10.1182/blood-2003-08-2765
72. Appay V, Zaunders JJ, Papagno L, Sutton J, Jaramillo A, Waters A, et al. Characterization of CD4(+) CTLs ex vivo. *J Immunol* (2002) 168:5954–8. doi: 10.4049/jimmunol.168.11.5954
73. Phetsouphanh C, Aldridge D, Marchi E, Munier CML, Meyerowitz J, Murray L, et al. Maintenance of functional CD57+ cytolytic CD4+ T cells in HIV+ elite controllers. *Front Immunol* (2019) 10:1844. doi: 10.3389/fimmu.2019.01844
74. Juno JA, van Bockel D, Kent SJ, Kelleher AD, Zaunders JJ, Munier CM. Cytotoxic CD4 T cells—friend or foe during viral infection? *Front Immunol* (2017) 8:19. doi: 10.3389/fimmu.2017.00019
75. Thevarajan I, Nguyen THO, Koutsakos M, Druce J, Caly L, van de Sandt CE, et al. Breadth of concomitant immune responses prior to patient recovery: a case report of non-severe COVID-19. *Nat Med* (2020) 26:453–5. doi: 10.1038/s41591-020-0819-2
76. Anderson P, Nagler-Anderson C, O'Brien C, Levine H, Watkins S, Slayter HS, et al. A monoclonal antibody reactive with a 15-kDa cytoplasmic granule-associated protein defines a subpopulation of CD8+ T lymphocytes. *J Immunol* (1990) 144:574–82.
77. Zhang JY, Wang XM, Xing X, Xu Z, Zhang C, Song JW, et al. Single-cell landscape of immunological responses in patients with COVID-19. *Nat Immunol* (2020) 21:1107–18. doi: 10.1038/s41590-020-0762-x
78. Jaimes JA, Millet JK, Whittaker GR. Proteolytic cleavage of the SARS-CoV-2 spike protein and the role of the novel S1/S2 site. *iScience* (2020) 23:101212. doi: 10.1016/j.isci.2020.101212
79. Hoffmann M, Kleine-Weber H, Schroeder S, Kruger N, Herrler T, Erichsen S, et al. SARS-CoV-2 cell entry depends on ACE2 and TMPRSS2 and is blocked by a clinically proven protease inhibitor. *Cell* (2020) 181:271–280 e278. doi: 10.1016/j.cell.2020.02.052
80. Essalmani R, Jain J, Susan-Resiga D, Andreo U, Evagelidis A, Derbali RM, et al. Distinctive roles of furin and TMPRSS2 in SARS-CoV-2 infectivity. *J Virol* (2022) 96(8):e0012822. doi: 10.1128/jvi.00128-22
81. Russell SM, Liew FY. T Cells primed by influenza virion internal components can cooperate in the antibody response to haemagglutinin. *Nature* (1979) 280:147–8. doi: 10.1038/280147a0
82. Scherle PA, Gerhard W. Functional analysis of influenza-specific helper T cell clones *in vivo*. T cells specific for internal viral proteins provide cognate help for B cell responses to hemagglutinin. *J Exp Med* (1986) 164:1114–28. doi: 10.1084/jem.164.4.1114
83. Sette A, Moutaftsi M, Moyron-Quiroz J, McCausland MM, Davies DH, Johnston RJ, et al. Selective CD4+ T cell help for antibody responses to a large viral pathogen: deterministic linkage of specificities. *Immunity* (2008) 28:847–58. doi: 10.1016/j.immuni.2008.04.018
84. Sztain T, Ahn SH, Bogetti AT, Casalino L, Goldsmith JA, Seitz E, et al. A glycan gate controls opening of the SARS-CoV-2 spike protein. *bioRxiv* (2021). doi: 10.1101/2021.02.15.431212
85. Li B, Deng A, Li K, Hu Y, Li Z, Shi Y, et al. Viral infection and transmission in a large, well-traced outbreak caused by the SARS-CoV-2 delta variant. *Nat Commun* (2022) 13:460. doi: 10.1038/s41467-022-28089-y
86. Grifoni A, Sidney J, Vita R, Peters B, Crotty S, Weiskopf D, et al. SARS-CoV-2 human T cell epitopes: Adaptive immune response against COVID-19. *Cell Host Microbe* (2021) 29:1076–92. doi: 10.1016/j.chom.2021.05.010
87. Mentzer AJ, O'Connor D, Bibi S, Chelysheva I, Clutterbuck EA, Demissie T, et al. Human leukocyte antigen alleles associate with COVID-19 vaccine immunogenicity and risk of breakthrough infection. *Nat Med* (2022). doi: 10.1038/s41591-022-02078-6

## COPYRIGHT

© 2022 Phetsouphanh, Khoo, Jackson, Klemm, Howe, Aggarwal, Akerman, Milogiannakis, Stella, Rouet, Schofield, Faulks, Law, Danwilai, Starr, Munier, Christ, Singh, Croucher, Brilot-Turville, Turville, Phan, Dore, Darley, Cunningham, Matthews, Kelleher and Zaunders. This is an open-access article distributed under the terms of the [Creative Commons Attribution License \(CC BY\)](https://creativecommons.org/licenses/by/4.0/). The use, distribution or reproduction in other forums is permitted, provided the original author(s) and the copyright owner(s) are credited and that the original publication in this journal is cited, in accordance with accepted academic practice. No use, distribution or reproduction is permitted which does not comply with these terms.